# Electrospun Scaffolds for Cartilage Tissue Engineering: Methods to Affect Anisotropy, Material, and Cellular Infiltration

by

Ned William Garrigues II

Department of Biomedical Engineering
Duke University

Date:_____

Approved:

_____
Farshid Guilak, Supervisor

_____
Louis E. DeFrate

_____
Kam W. Leong

_____
Lori A. Setton

_____
George A. Truskey

Dissertation submitted in partial fulfillment of
the requirements for the degree of Doctor of Philosophy in the Department of
Biomedical Engineering in the Graduate School
of Duke University

2011

ABSTRACT

Electrospun Scaffolds for Cartilage Tissue Engineering:
Methods to Affect Anisotropy, Material, and Cellular Infiltration

by

Ned William Garrigues II

Department of Biomedical Engineering
Duke University

Date:_____
Approved:

_____
Farshid Guilak, Supervisor

_____
Louis E. DeFrate

_____
Kam W. Leong

_____
Lori A. Setton

_____
George A. Truskey

An abstract of a dissertation submitted in partial
fulfillment of the requirements for the degree
of Doctor of Philosophy in the Department of
Biomedical Engineering in the Graduate School
of Duke University

2011

# Abstract

The aim of this dissertation was to develop new techniques for producing electrospun scaffolds for use in the tissue engineering of articular cartilage. We developed a novel method of imparting mechanical anisotropy to electrospun scaffolds that allowed the production of a single, cohesive scaffold with varying directions of anisotropy in different layers by employing insulating masks to control the electric field. We improved the quantification of fiber alignment, discovering that surface fibers in isotropic scaffolds show similar amounts of fiber alignment as some types of anisotropic scaffolds, and that cells align themselves in response to this subtle fiber alignment. We improved previous methods to improve cellular infiltration into tissue engineering scaffolds. Finally, we produced a new material with chondrogenic potential consisting of native unpurified cartilage which was electrospun as a composite with a synthetic polymer. This work provided advances in three major areas of tissue engineering: scaffold properties, cell-scaffold interaction, and novel materials.

# Dedication

To my wife, Sarah.

# Contents

# List of Figures

## Acknowledgements

I would like to thank my advisor, Dr. Farshid Guilak, for bringing me into his lab and giving me the flexibility to solve problems however I saw fit. I appreciate the faith that he had in me to get a new project off the ground. Thank you to my committee members, Drs. Lou DeFrate, Lori Setton, Kam Leong, and George Truskey, for their input and advice in proposing this dissertation.

I have grown considerably as a scientist and a person with the help of the members of the Orthopaedic Bioengineering Laboratory. I am thankful that Dianne Little appreciated the potential of electrospinning, as she has provided me immeasurable guidance in my work as we tackled many of the same problems. Brian Diekman and Chia-Lung Wu brought me up to speed on chondrogenic cell culture and were always generous with their time, expertise, and supply stockpiles. Holly Leddy, Amy McNulty, and Bridgette Furman served as an amazing sounding board for questions and complaints about science, statistics, and graduate school. Jonathan Brunger has been supportive, insightful, prepared with a late night pep talk, and he has always appreciated my contributions to the lab that were otherwise overlooked. Thanks to Ian Gao and Jason Klein for working so diligently and carefully on this project even while we were struggling. I would particularly like to thank John Finan for his amazing

ideas, clear thinking, creativity, and scientific insight, as well as being a friend and mentor.

My parents, Ned and Maxine, taught me science from a young age and taught me always to take the most rigorous road. My brother, Grant, has consistently been a role model. He encouraged me to come to Duke and loves talking shop (to the occasional irritation of our wives). I hold out hope that we will join forces to work together on orthopaedic challenges again in the future. Finally, I would like to thank my wife, Sarah. She was patient with me when I got home from lab in the middle of the night, and she motivated me when I struggled. She carried me through the toughest times of my graduate school career, inspired me to keep going, and made me excited for the phase of our lives where I no longer carry the job title "student

# 1. Background and Significance

## *1.1 Cartilage Tissue Engineering*

### 1.1.1 Structure and Function of Articular Cartilage

Articular cartilage is a load-bearing tissue that covers the articulating surfaces of diarthrodial joints. It is deformable and serves to lower contact stresses by distributing loads across the joint, as well as to increase joint congruity.(Mow, Ratcliffe et al. 1992; Mow, Ateshian et al. 1993) It allows joint movement with minimal resistance and wear.

Cartilage is a hydrated connective tissue, consisting of 68-85% water when in its natural state. Collagen (primarily collagen II) makes up 10-20% of the mass, while proteoglycans are 5-10%. Thus, it is avascular, aneural, and alymphatic, and has only a relatively small population of cells, called chondrocytes.(Mow and Guo 2002; Mow and Huiskes 2005) These cells maintain and remodel the tissue, but do not exhibit any significant capacity for repair. Damage can result from local injury or systemic disease (osteoarthritis), causing focal defects and large-scale degeneration. This damage is not healed, and is intensified through repeated loading and wear, leading to further damage, pain, loss of mobility, and therefore decreased quality of life for the patient.

### 1.1.2 Mechanical Properties of Articular Cartilage

Cartilage has mechanical properties that are anisotropic, inhomogeneous, nonlinear, and viscoelastic.(Huang, Stankiewicz et al. 1999; Mow and Guo 2002; Verteramo and Seedhorn 2004) Its low coefficient of friction can withstand wear over

the life of most joints. Cartilage is often modeled as a biphasic system. Briefly, the proteoglycans hold negative charges, which attract water, resulting in an osmotic pressure. As the tissue is compressed, the water is extruded through the pores of the tissue, with some remaining inside the tissue due to the Donnan osmotic pressure. The fluid pressure from this remaining water holds roughly 95% of the compressive load in the tissue, and functions to convert the compressive loads on the tissue as a whole into tensile loads in the collagen II fibrils that make up the majority of the dry weight of cartilage. This pressurization means that cartilage-cartilage friction is only 5% of what it would be in the absence of fluid pressure. This fluid pressurization, as well as the slow extrusion of the water from the tissue, gives cartilage its viscoelastic behavior. The viscoelastic behavior allows energy dissipation through friction of the fluid flow, as well as deformation of some of the molecules.(Mak 1986; Mow and Guo 2002) Additionally, the viscoelastic properties allow much better load distribution. If cartilage were truly elastic, it would require a higher modulus, leading to areas of contact that show high compressive stresses, mitigated only partially by the increasing contact area from the deformation. However, the viscoelastic nature allows fluid flow to distribute the load across the contact area much more evenly.

The collagen fibrils are arranged in an inhomogeneous and anisotropic manner. The surface zone has fibers oriented parallel to the surface, and the fiber orientation transitions through the middle zone to the deep zone and the tidemark where the fibers

are oriented normal to the articular surface.(Ateshian and Hung 2003) These fibril arrangements are visible at a macroscopic level because they form split lines when pricked with a needle.(Below, Arnoczky et al. 2002) Additionally, these split lines indicate the presence of anisotropy and which direction is the stiffest. For example, cartilage on the humeral head has a tensile modulus of 7.8 MPa in the direction of the split lines, and 5.9 MPa perpendicular to them. Therefore, the cartilage was 32-35% stiffer in the split line direction. This anisotropy was maintained throughout the thickness and increased to 63% in the surface zone at 0.16 strain.(Huang, Stankiewicz et al. 1999) Other published results are similar, but some indicate that the anisotropy causes stiffness up to 3 times higher in one direction than another.(Kempson, Freeman et al. 1968; Woo, Akeson et al. 1976; Verteramo and Seedhorn 2004)

### 1.1.3 The need for cartilage repair

Some estimates indicate that more than 20 million Americans suffer from osteoarthritis, costing more than $60 billion annually in the US in treatment costs. In addition to these medical costs, there is substantial productivity loss, as work limitations due to arthritis affect 5% of the US population, arthritis being the most common cause of disability. Osteoarthritis is the most prevalent form of arthritis, with more than 60% of Americans over the age of 60 living with osteoarthritis and the lifetime risk for knee osteoarthritis being 46%. Osteoarthritis's prevalence in older patients makes it a growing problem for the United States, with the impending growth of the size of the

over-60 population. Additionally, obese patients and patients who sustained joint injuries at a young age are at risk. These risk groups are also growing as obesity rates rise and youth sports injuries become more common.(Buckwalter, Saltzman et al. 2004; Buckwalter and Martin 2006; CDC 2011; NIAMS 2011)

### 1.1.4 Current clinical repair strategies

Currently, the standard of care for severe osteoarthritis is total joint arthroplasty. This procedure is highly invasive, and often lasts only 10-15 years before a difficult revision surgery is necessary.(NIAMS 2011) This is highly problematic, as increasing numbers of younger patients with severe osteoarthritis due to joint injuries or obesity need mobility and pain relief for considerably longer than the lifetime of a total joint implant. These patients often suffer over long periods of time in an attempt to delay surgery for as long as possible.

Alternatives to total joint arthroplasty represent moderately successful attempts at replacing or regenerating cartilage tissue, but do not adequately recreate the tissue, leaving substantial room for improvement. Autologous tissue transplantation involves removing cylindrical osteochondral samples from a non-load-bearing portion of the cartilage and implanting them at the site of a focal defect. Larger defects are treated with mosaicplasty, in which multiple samples of autologous tissue are implanted near each other.(Hangody, Kish et al. 1997) However, this technique produces fibrocartilage in the areas between the round implants unfilled with cartilage and certainly does not

restore the original nature of the smooth cartilage, in addition to causing donor site morbidity.

Other methods to treat osteoarthritis involve providing a new cell population to the site. The most common of these is cell recruitment via microfracture, in which holes are drilled into the subchondral bone, prompting bleeding and the recruitment of mesenchymal stem cells and other cell populations from the bone marrow.(Steadman, Rodkey et al. 2001) A newer treatment involves the implantation of autologous chondrocytes isolated from non-load-bearing cartilage and expanded *in vitro* using periosteum to confined the cells and possibly provide cellular signals to promote tissue growth, which initially showed good results, but randomized clinical trials showed no outcomes similar to microfracture.(Coleman, Malizia et al. 2001; Wood, Malek et al. 2006; Knutsen, Drogset et al. 2007) These surgical treatments often produce fibrocartilage, rather than the hyaline cartilage present in healthy joints, providing different mechanical properties and possibly less long-term stability.

It is clear that cartilage is an excellent target for tissue engineering due to the large number of patients requiring treatment for osteoarthritis. Implantation of engineered cartilage would allow surgical intervention that could alleviate much of the pain and loss of mobility that is associated with osteoarthritis, without the large osteotomy that accompanies arthroplasty. As a step towards the engineering of articular

cartilage, this dissertation will focus on using electrospinning techniques to produce scaffolds for tissue engineering of articular cartilage.

## *1.2 Electrospinning*

### 1.2.1 Electrospinning

Electrospun scaffolds are excellent candidates for use in the tissue engineering of articular cartilage. These scaffolds can be made with a number of different polymers and can be produced to have fibers with submicron diameters. Electrospinning is a technique for creating nanofibers and nanofibrous meshes using high voltage to draw out a polymer. Nearly any polymer can be used, provided that the polymer can be made into a solution or melt, which allows an enormous amount of flexibility in production. The process does not require an extensive apparatus, as the basic design is unchanged since it was first patented in 1934.(Formhals 1934)

Electrospun scaffolds have been used for various applications, such as filters, wound dressings, and fiber-reinforced composites.(Kim and Reneker 1999; Li and Xia 2004) This method of scaffold production utilizes a strong electric potential difference between a collecting electrode and a needle positioned a short distance away, slowly ejecting a viscous polymer solution. This produces randomly aligned fibers with diameters of 3 nm – 5 μm.(Pham, Sharma et al. 2006) It should be noted that the electrospinning process aligns the polymer chains within the fiber, resulting in stronger fibers at small sizes.(Jaeger, Schischka et al. 2009)

A polymer (polycaprolactone, in these experiments), is dissolved in a solvent, and then placed in a syringe with an electrically conductive needle. An electrode is attached to the needle and a large (5-30 kV) potential difference is applied between it and a collecting electrode which is placed 5-30 cm away. Charges accumulate in the polymer and are attracted towards the collector. As the voltage is increased, a cone shape (the Taylor Cone), as visible in Figure 1, develops as the charges try to reach a low-energy conformation by approaching the low potential, yet still avoiding the other charges in the solution.(Taylor 1964; Taylor 1969; Ramakrishna, Fujihara et al. 2005)

If the viscosity of the solution is high enough, the polymer solution is drawn out into a fiber as it flies through a high electric field toward the collecting electrode. As the jet is drawn to the collector, the fibers are at an unstable equilibrium relative to the center axis of the needle. When they are perturbed off of the center axis, the like charges elsewhere in the jet repel each other with coulombic forces generated by the strong electric field, driving the jet farther off-center. This whipping instability produces the random quality of the resulting fiber mat, and draws the fiber out much farther, producing nanoscale fibers.(Doshi and Reneker 1995; Reneker, Yarin et al. 2000; Ramakrishna, Fujihara et al. 2005) Fiber size and morphology can be controlled by varying the concentration, solvent system, flow rate, needle size, electric field strength, electric field shape, or distance, in addition to ambient parameters such as temperature and humidity.

### 1.2.2 Electrospinning for Tissue Engineering

Electrospun scaffolds are an excellent candidate for the tissue engineering of articular cartilage. Electrospun fibers, which can be as small as 3 nm in diameter, are much closer in size to collagen fibers than the fibers or surface features of other scaffolds used for tissue engineering. It is thought that the small fiber diameter will promote favorable interactions between cells and the scaffold. The small fiber size gives a high surface area to volume ratio, which likely favors cell attachment.

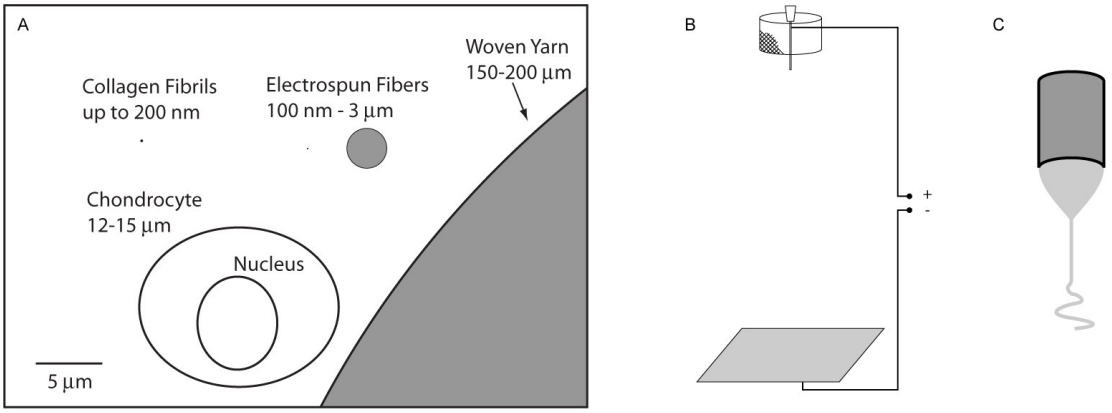


**Figure 1: (A) Scale of electrospun fiber and woven fiber relative to chondrocytes showing that electrospun fibers interact as small fibers, whereas woven fibers can be considered locally flat relative to the chondrocyte. (B) Schematic of basic electrospinning setup. Polymer solution is pumped through the needle on the syringe, which has a round mesh focusing cage attached to it. The needle is held at high voltage and the collecting electrode at ground. (C) Close-up of needle tip, showing Taylor cone and electrospinning jet.**

Recently, electrospun scaffolds have become widely used as a scaffold for tissue engineering, because they have shown promise in the engineering of many tissues, including cartilage, meniscus, tendon, bone, fat, and muscle.(Li, Tuli et al. 2005; Li, Mauck et al. 2007; Choi, Lee et al. 2008; Kumbar, James et al. 2008; McCullen, Zhu et al.

2009) This growth in research stems from the scaffold's controllable properties and versatile applications. The scaffolds can be made of proteins, have hollow fibers that can hold cells, release drugs controllably, or be chemically functionalized.(Shields, Beckman et al. 2004; Li, McCann et al. 2005; Jayasinghe and Townsend-Nicholson 2006; Dong, Arnoult et al. 2009) Electrospun scaffolds can be produced with nearly any polymer, have controllable fiber diameter, and support cell attachment and proliferation.(Deitzel, Kleinmeyer et al. 2001; Li, Laurencin et al. 2002; Lee, Kim et al. 2003; Xie, Li et al. 2008) Further, the nanoscale fiber size prompts a diminished foreign body response *in vivo* (Sanders, Stiles et al. 2000; Sanders, Cassisi et al. 2003), and has advantageous effects on the phenotype of chondrocytes cultured on electrospun scaffolds.(Li, Danielson et al. 2003; Li, Jiang et al. 2006)

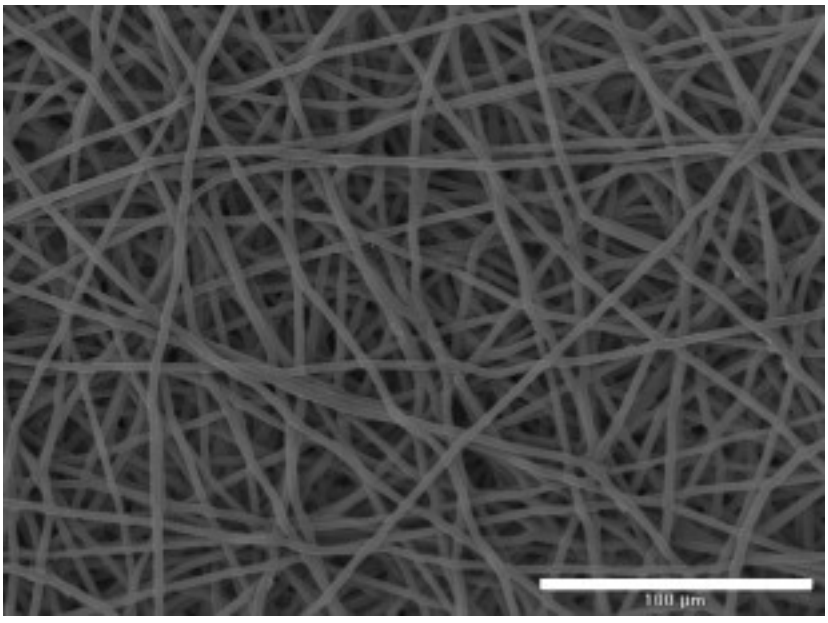


**Figure 2: Scanning electron microscope image of an electrospun scaffold. Note the tiny pores. Scale bar: 100µm**

Additionally, electrospun scaffolds can have their mechanical properties tailored to the specific application. Polymers can be chosen for hydrophilicity, degradation rate, modulus, immune response, or any other of a number of parameters. The described work uses poly(ε-caprolactone) (PCL), which has an adequately long degradation time *in vivo*, up to 3 years, though the molecular weight decays exponentially.(Sun, Mei et al. 2006) It is possible that varying the fiber diameter in an electrospun scaffold will affect the permeability and thus, the viscoelastic behavior. This ability to tailor the mechanical properties of the scaffold is crucial in the tissue engineering of a biomechanical tissue, because it allows the scaffold to function as the tissue until the cell population can take over the role.

Finally, there are many recent advances in electrospinning that could be harnessed for tissue engineering. Coaxial fibers have been produced for controlled drug release. Coaxial needles can be used to make a fiber with a core rich in a drug and a sheath with small pores, allowing slow drug release. (Chew, Wen et al. 2005; Li, Ouyang et al. 2005; Jayasinghe and Townsend-Nicholson 2006; Liao, Chew et al. 2006; Luong-Van, Grondahl et al. 2006; Chakraborty, Liao et al. 2009; Liao, Chen et al. 2009) Even proteins such as collagen have been electrospun, which would be helpful in the pursuit of tissue engineered cartilage. (Matthews, Wnek et al. 2002; Boland, Matthews et al. 2004; Shields, Beckman et al. 2004; Buttafoco, Kolkman et al. 2006)

### 1.2.3 Anisotropy

Prior research has focused on creating electrospun scaffolds that exhibit mechanical anisotropy, or mechanical properties that vary with direction. This focus is largely the result of the functional tissue engineering approach, a movement within the field of tissue engineering supporting selection of scaffolds for tissue engineering which have properties that approximate the native tissue in some key aspects, including anisotropy.(Butler, Goldstein et al. 2000) Mechanical anisotropy is especially important for musculoskeletal tissues, because the principal role of these tissues is mechanical. This concept has spurred research to engineer anisotropic electrospun scaffolds that are stiffer in one direction than another.(Yin, Chen et al.; Courtney, Sacks et al. 2006; Nerurkar, Baker et al. 2006; Baker and Mauck 2007; Nerurkar, Elliott et al. 2007) In addition to the stiffness of the scaffold, the alignment of nanofibers has even been shown to affect the cell phenotype and the structure of the deposited proteins.(Yin, Chen et al.; Baker and Mauck 2007) When cultured with cells, alignment of surface topology, such as aligned electrospun fibers, enhances the alignment of the cells as well as the structural integrity of the extracellular matrix deposited by the cells.(Yim, Reano et al. 2005; Chew, Mi et al. 2008; Hwang, Park et al. 2009) Aligned fibers can also induce functional improvements, such as electrophysiological recovery in a nerve-injury model.(Chew, Mi et al. 2007) Interest in anisotropic scaffolds is broad, including anisotropic woven scaffolds (Moutos, Freed et al. 2007) and various methods to align electrospun fibers.

Previous research has shown that increased levels of fiber alignment result in increased mechanical anisotropy. (Ayres, Bowlin et al. 2006; Ayres, Bowlin et al. 2007; Li, Mauck et al. 2007; Ayres, Jha et al. 2008) Methods to create anisotropy are varied and provide mixed results. One technique relies on the use of collecting electrodes with insulators interspersed, producing extremely well aligned fibers that orient across the insulating gap.(Li, Wang et al. 2003; Li, Wang et al. 2004; Li, Ouyang et al. 2005) This process has been successfully scaled up to produce three different aligned directions. However, this technique produced only a small number of aligned fibers, and was not extended to make a scaffold with substantial mechanical integrity. In fact, when this technique is continued long enough to make a thick scaffold, an inhomogeneous macroscale texture appears, most likely due to charge buildup, making it unsuitable for a low-friction tissue like cartilage. A second method of alignment, which utilizes a collecting electrode moving back and forth, allows multiple directions of alignment;(Kim 2008) however, this system is quite costly because in involves a rapidly moving controllable stage, and has not been substantially pursued. Scaffolds have been aligned after production by using heat during tensile loading.(Zong, Bien et al. 2005) Further efforts to align the fibers have focused on collecting the fibers on a rapidly spinning mandrel, physically pulling the fibers into alignment.(Liao, Chew et al. 2006; Nerurkar, Baker et al. 2006; Baker and Mauck 2007; Chew, Mi et al. 2007; Nerurkar, Elliott et al. 2007; Chew, Mi et al. 2008; Baker, Nathan et al. 2009) Sometimes, a separate,

attracting electrode is added behind the mandrel to improve the alignment.(Carnell, Siochi et al. 2008) The main drawback with this technique is that it allows only one preferred fiber direction in the scaffold. Additional directions can only be achieved by removing the scaffold from the mandrel and then reattaching it at a different angle, which is problematic because the successive layers do not adhere together well.

Current methods in the literature fall short of imitating each of the unique properties of individual layers of human tissue in the construction of the tissue's layers. To better approximate human tissue, it is necessary to create scaffolds exhibiting mechanical anisotropy, so that each layer's properties can be independently controlled based on the type of tissue being grown.

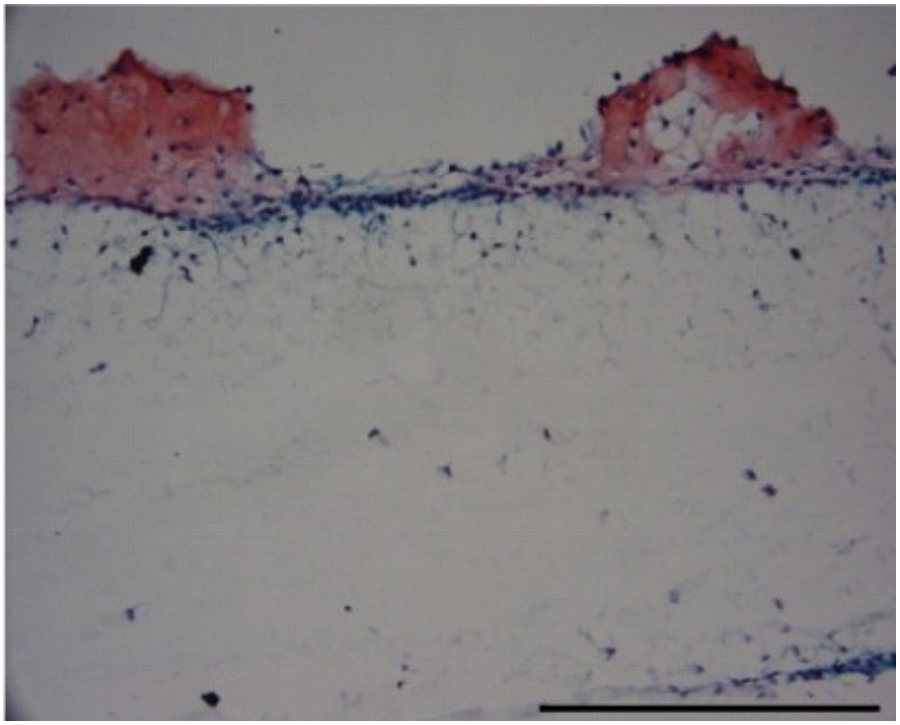

**Figure 3: Chondrocyte infiltration after 28 days in culture. Note how very few cells are in the center of the scaffold. Hematoxylin, Safranin O, Fast Green stain. Scale bar: 250 μm.**

### 1.2.4 Cellular Infiltration

Electrospun scaffolds are highly porous, giving ample room for cells to attach, and the fibers are small enough that cells can push the fibers aside to expand small pores.(Li, Laurencin et al. 2002) These pores are extremely interconnected, allowing easy diffusion of culture media and nutrients throughout the scaffold. This is an important feature during the culture of the scaffolds and after implantation, as it allows the cell population inside to be maintained in static culture and in the joint through simple equilibration with the surrounding environment.

On the other hand, the pores of electrospun scaffolds are too small for cell seeding. The majority of pores are 25-100 μm (Li, Laurencin et al. 2002), which is sufficient for cell migration, but not for macroscale seeding. The cells can slide through the pores slowly, moving the tiny fibers out of the way as they migrate into the scaffold. However, the cells will not simply flow into the scaffold with the fluid, rendering seeding by simple pipetting or vacuum infusion ineffective. Migration into the scaffold is greatly retarded by the diffusional advantage that the cells have when they are on the surface, where they have access to all of the nutrients in the media and where waste products are carried away almost instantly. The cells have greater access to nutrients on the surface of the scaffold than they do in the interior and therefore will not migrate quickly or in substantial numbers. Efforts to seed using vacuum infusion (Chen, Michaud et al. 2009) or varied fiber diameter to increase pore size (Pham, Sharma et al. 2006) have improved infiltration, but are still inadequate to get cells through the entire scaffold without the aid of vacuum perfusion culture. Another method involves using a water bath as the grounded collecting electrode, allowing the production of a scaffold composed of multiple thin layers which were expanded by drying in a vacuum.(Tzezana, Zussman et al. 2008) These scaffolds had superior infiltration compared to the single-layered electrospun scaffolds that are typically used in tissue engineering, but scaffolds like these have extremely low fiber density and

Therefore, much of the tissue engineering work on electrospun scaffolds has shown insufficient cellular infiltration to be considered a functional tissue. (Li, Laurencin et al. 2002; Li, Danielson et al. 2003; Li, Mauck et al. 2005; Li, Tuli et al. 2005; Li, Jiang et al. 2006; Li, Mauck et al. 2007)

It is clear the electrospinning represents a promising technique for producing tissue engineering scaffolds. The described work seeks to do the following:

- Develop a method for anisotropic electrospinning that can be applied to produce a scaffold with multiple layers of differing anisotropy.
- Improve methods to distribute cells throughout the thickness of electrospun scaffolds.
- Incorporate native cartilage proteins into electrospun scaffolds.

## *1.3 Hypothesis and Aims*

The described work consists of the development of scaffolds for the tissue engineering of cartilage. We sought to produce electrospun polymer scaffolds to be seeded with a population of cells that then deposit collagens and proteoglycans, forming the extracellular matrix that provides the mechanical properties necessary to sustain and distribute loads. This scaffold degrades slowly over time, leaving the new cartilaginous tissue, which is maintained and remodeled by the cell population.

**The goal of this project was to advance the use of electrospinning for scaffold production in the pursuit of tissue engineered cartilage. The focus was upon the mechanical properties of the scaffold as well as the cellular response to the structure and new materials of the scaffold.**

***Specific Aim 1***: *Produce electrospun scaffolds with controllable mechanical anisotropy, having multiple layers of varied orientation incorporated into a single, cohesive scaffold.* Current methods of imparting mechanical anisotropy to scaffolds only allow one preferred direction. We designed a new electrospinning technique that allows controllable mechanical anisotropy in multiple layers while maintaining the mechanical integrity of the scaffold as a whole. This anisotropy is comparable to the anisotropy of native articular cartilage. We investigated whether this level of anisotropy influences the alignment of cells grown on the scaffold.

***Specific Aim 2***: *Improve cellular infiltration of electrospun scaffolds by changing the scaffold structure.* Electrospun scaffolds do not allow sufficient cell infiltration for eventual tissue replacement. Therefore, we studied hydrospinning as a method for electrospinning scaffolds for tissue engineering that allow cell infiltration and tissue growth throughout the thickness of the scaffold.

***Specific Aim 3***: *Develop electrospun scaffolds that incorporate native cartilage proteins to improve cartilage-specific matrix synthesis.* We investigated new materials for cartilage tissue engineering with electrospun scaffolds, specifically the incorporation of

native cartilage proteins. We examined whether these materials maintain their protein structure, induce chondrogenic effects in the cells, and result in a more cartilaginous engineered tissue

# 2. Use of an insulating mask for controlling anisotropy in multilayer electrospun scaffolds for tissue engineering[1]

## *2.1 Introduction*

Tissue engineering seeks to apply combinations of cells, biomaterial scaffolds, and bioactive molecules to enhance the repair or regeneration of injured or diseases tissues. Despite many rapid advances, challenges still remain with respect to the development of functional replacements for tissues that primarily serve a biomechanical role, such as musculoskeletal tissues.(Butler, Goldstein et al. 2000) In this regard, the mechanical properties of the biomaterial scaffold can play an important role in the success of the engineered tissue not only by providing structural support during early phases of tissue regeneration, but also by influencing cell alignment, tissue growth, and differentiation through physical interactions with cells.(Guilak, Cohen et al. 2009) In particular, recent studies suggest that the size and orientation of nanoscale structures within a biomaterial scaffold may have a significant influence on cell behavior and alignment.(Li, Tuli et al. 2005; Yim, Reano et al. 2005; Li, Jiang et al. 2006; Baker and Mauck 2007; Li, Mauck et al. 2007; Chew, Mi et al. 2008; Choi, Lee et al. 2008) Therefore, the ability to define scaffold architecture at multiple length scales may provide novel means of enhancing cell-based tissue engineering.

---

[1] Reprinted with permission from Garrigues, N.W., et al., *Use of an insulating mask for controlling anisotropy in multilayer electrospun scaffolds for tissue engineering.* J Mater Chem. **20**(40): p. 8962-8968.

Electrospun scaffolds have shown promise in the engineering of many tissues, including cartilage, meniscus, tendon, bone, fat, heart valve, intervertebral disc, and muscle.(Li, Tuli et al. 2005; Courtney, Sacks et al. 2006; Pham, Sharma et al. 2006; Christenson, Anseth et al. 2007; Li, Mauck et al. 2007; Choi, Lee et al. 2008; Kumbar, James et al. 2008; Stella, Liao et al. 2008; Mauck, Baker et al. 2009; McCullen, Zhu et al. 2009) The scaffolds can be engineered to have controllable and versatile properties, such as hollow fibers containing cells, controllable drug release, or chemical functionalization.(Shields, Beckman et al. 2004; Li, McCann et al. 2005; Jayasinghe and Townsend-Nicholson 2006; Dong, Arnoult et al. 2009) Electrospun scaffolds can be produced using nearly any polymer, have controllable fiber diameter, and support cell attachment and proliferation.(Deitzel, Kleinmeyer et al. 2001; Li, Laurencin et al. 2002; Lee, Kim et al. 2003; Xie, Li et al. 2008) Further, the nanoscale fiber size prompts a diminished foreign body response *in vivo*, and has advantageous effects on the phenotype of chondrocytes cultured on electrospun scaffolds.(Sanders, Stiles et al. 2000; Li, Danielson et al. 2003; Sanders, Cassisi et al. 2003; Li, Jiang et al. 2006)

Because electrospinning of nanofibers onto a collecting plate produces a randomly aligned scaffold, efforts to apply electrospun scaffolds to the mechanical requirements of various engineered tissues have focused on the introduction of mechanical anisotropy (mechanical properties that vary with direction) into the scaffold.(Yin, Chen et al.; Courtney, Sacks et al. 2006; Nerurkar, Baker et al. 2006; Baker

and Mauck 2007; Nerurkar, Elliott et al. 2007) In addition to the stiffness of the scaffold, the alignment of nanofibers has even been shown to affect cell alignment and phenotype, as well as the structure of the deposited extracellular matrix.(Yin, Chen et al.; Yim, Reano et al. 2005; Baker and Mauck 2007; Li, Mauck et al. 2007; Chew, Mi et al. 2008; Kim 2008; Hwang, Park et al. 2009; Cao, Mchugh et al. 2010) Interest in anisotropic scaffolds is broad, including anisotropic woven scaffolds,(Moutos, Freed et al. 2007) and methods to align electrospun fibers.(Mauck, Baker et al. 2009) Various techniques to create anisotropy have been used and include moving the collector electrode to physically pull the fibers into alignment, typically by collecting fibers on a rapidly spinning mandrel.(Nerurkar, Baker et al. 2006; Baker and Mauck 2007; Nerurkar, Elliott et al. 2007; Carnell, Siochi et al. 2008; Baker, Nathan et al. 2009) This technique is successful in producing highly anisotropic scaffolds for tissue engineering, but does not directly allow the formation of multilayered scaffolds with differing anisotropy; rather, individual aligned layers must be removed and combined, or cultured to form a composite using deposited extracellular matrix *in vitro*.(Nerurkar, Baker et al. 2009) Another method to align fibers involves shaping the electrodes and interspersing insulators to collect the fibers that align across the insulating gap.(Li, Wang et al. 2003; Li, Wang et al. 2004; Li, Ouyang et al. 2005) This method produces highly aligned fibers but is not suitable for making thick scaffolds that are often required for tissue engineering. Further, current methods for creating anisotropy in electrospun scaffolds

are unable to imitate the unique properties of individual layers of human tissue in the construction of each layer of the scaffold. To better approximate the nano- and micro-scale architecture of different tissues, it is necessary to create scaffolds with controlled mechanical anisotropy, so that the properties of each layer can be independently controlled based on the type of tissue being grown.

In this study, we developed a method for creating a multilayered electrospun scaffold, with each layer having its own preferred fiber direction, without requiring lamination for consolidation of the different layers. We used rectangular and square insulating masks to control the geometry of the electric field, which controls the alignment of the deposited fibers and generates mechanical anisotropy in the resulting scaffold. We analyzed fiber alignment, the tensile mechanical properties in two orthogonal directions, and alignment of adipose stem cells when cultured on the scaffolds.

## *2.2 Materials and Methods*

### 2.2.1 Electrospinning

Poly(ε-caprolactone) (PCL) ($M_n$=42,500, $M_w$=65,000) (Sigma Aldrich, St. Louis, MO) was dissolved at 15% (w/v) in a solvent of 70% (v/v) dichloromethane (Sigma Aldrich, St. Louis, MO) and 30% ethanol at room temperature overnight. The PCL solution was pumped with a syringe pump (Cole-Parmer Instrument Co., 74900-00, Vernon Hills, IL) through a blunt-tip 25 gauge needle with a round focusing cage (3 cm

diameter, 4 mm above end of needle tip) at 4 ml/hr across a 14 cm gap with 20 kV applied (Gamma High Voltage Research, Ormond Beach, FL) for 7 minutes. The pump was turned off at this time and the system was given 4 minutes to stop electrospinning due to the residual pressure in the pump. The collecting electrode was a 12.5 cm square flat copper plate, with a polysiloxane rubber insulating mask placed on top (Figure 4). The rubber masks were 13.2 cm square, 0.16 cm thick, with a 25 $cm^2$ opening cut in the center. One mask had a square aperture (5 cm x 5 cm) (producing what we have termed "unaligned scaffolds"), and the other had a rectangular aperture (10 cm x 2.5 cm) (producing what we have termed "aligned scaffolds"), such that the two masks have exposed surfaces that are equal in area.

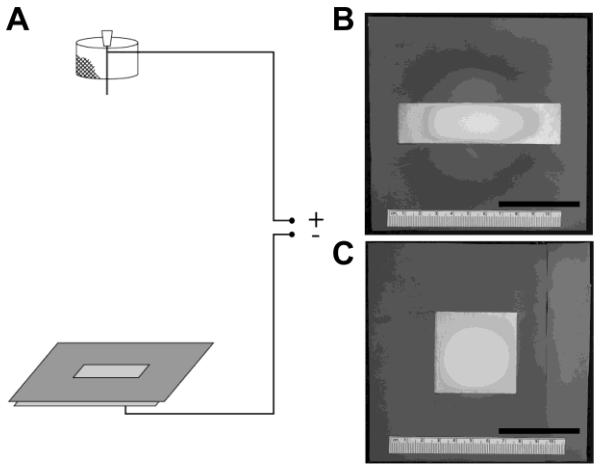


**Figure 4: (A) Electrospinning Apparatus. The copper collector electrode is covered by a rubber insulating mask with a 25$cm^2$ aperture. (B, C) Scaffolds on collector electrode with insulating masks *in situ*. (B) Rectangular mask and scaffold. Note the small amount of fibers collected on the mask. (C) Square mask and scaffold. Scale bar = 5cm.**

### 2.2.2 Mechanical Testing

Scaffolds were tested in tension in both the axial (parallel with the long axis of the rectangular mask or a given side of the square mask) and transverse directions (orthogonal to the axial direction). Scaffolds were prepared for mechanical testing by pre-wetting with PBS (pH 7.4). Because PCL is hydrophobic, samples were initially submerged in ethanol, and then graduated concentrations of ethanol/PBS until the samples were left in PBS overnight. Samples were cut with a dog-bone shaped die that had a central section 1 mm wide and 10 mm long. Tensile tests were performed in a universal testing machine (Bose EnduraTEC SmartTest, Eden Prairie, MN) with a 2 g tare load at 0.1% strain/sec, with strain data gathered using a digital camera (Sony XCD-X700, Tokyo, Japan) every 1 second. Thickness was calculated using an adjacent section of the scaffold and the camera, using digital calipers in Vision Builder (National Instruments, Austin, TX). True stress was determined by dividing the force by the cross-sectional area of the specimen, corrected for narrowing in width (Figure 6). All other data and calculations employed engineering stress and infinitesimal strain. A minimum of 11-13 scaffolds were tested from each group in each direction, for a total of n=47 scaffolds.

### 2.2.3 Fiber Alignment Measurement

The fast Fourier Transform (FFT) was used to analyze fiber orientation in the scaffolds, based on a modification of the technique reported previously.(Ayres, Bowlin

et al. 2006; Ayres, Bowlin et al. 2007; Ayres, Jha et al. 2008) One to three 6 mm punches were taken from each scaffold, at least 0.5 cm away from the edges. Using a scanning electron microscope (SEM) (FEI XL30 ESEM, Hillsboro, OR), at least 3 images of random, non-overlapping locations away from the edge were taken of each punch, yielding 4-9 images each scaffold (n=8-9 specimens per group) at 1000x magnification. Scaffolds were sputter-coated with gold and palladium (Desk IV, Denton Vacuum, Moorestown, NJ) before imaging. Image analysis was performed in MATLAB (MathWorks, Natick, MA) as follows: Images were cropped to a square, thresholded using Otsu's method, and then masked with a radial gradient to gray before a 2D fast Fourier Transform was applied. Pixel intensities were summed along the radius of the power spectrum, with bilinear interpolation, at intervals of 1°, then normalized by area and recentered on 0. Peaks due to pixel edges were automatically removed by replacing the data from the 5° on either side of 0° with a linear interpolation between the averages of the next 5° on either side. This was repeated at 90°. Profiles from each image of the same punch were averaged, and then the profiles from each punch of the same scaffold were averaged to get an overall profile for each scaffold. Data were normalized to show actual angle of alignment relative to the expected angle of alignment.

The data was analyzed in two ways. First, the average height of the profile for the 15° on either side of the expected orientation was designated the Fiber Alignment Index, with higher values meaning that the fibers within a scaffold were more aligned in

the expected direction. Second, the profile from each scaffold was fit using MATLAB to a sinusoid of the form $y=A*\sin(2x + \pi/2 + B)$ where A and B were the amplitude and phase shift, respectively, to examine the degree and direction of alignment without constraining analysis to the expected direction.

### 2.2.4 Multilayer Scaffolds

Multilayer scaffolds consisted of more than one layer of scaffold being produced using the rectangular mask in the same way as above, with each layer having a different mask orientation from the preceding layer. After 7 minutes of electrospinning to produce the first layer, the insulating mask was rotated 90° relative to the collecting electrode and attached scaffold, without stopping the electrospinning process. Scaffolds were produced with 2 layers and evaluated for fiber alignment as above.

### 2.2.5 Cell Alignment

Single layer scaffolds were cut to a round shape with a small straight edge in the expected alignment direction, then treated with 4 M NaOH for 18 hours to increase hydrophilicity before rinsing and sterilizing in ethanol with UV light. The scaffolds were then soaked with ethanol, then PBS, then incubated with fetal bovine serum (Zen-Bio, Research Triangle Park, NC) overnight at 37°C. These prepared scaffolds were then seeded with passage 5 adipose stem cells at 200,000 cells/$cm^2$.(Estes, Wu et al. 2006; Guilak, Lott et al. 2006) The constructs were cultured with expansion medium consisting of Dulbecco's Modified Eagle's Medium: Nutrient Mixture F-12 (Gibco, Grand Island,

NY), 10% fetal bovine serum (Zen-Bio, Research Triangle Park, NC), 1% penicillin-streptomycin (Invitrogen, Carlsbad, CA), 5 ng/ml recombinant human epidermal growth factor (Roche Diagnostics, Indianapolis, IN), 1 ng/ml recombinant human basic fibroblastic growth factor (Roche Diagnostics, Indianapolis, IN), and 0.25 ng/ml transforming growth factor-β1 (R&D Systems, Minneapolis, MN) for 4 days before being stained with Syto 13 nuclear stain (Invitrogen, Carlsbad, CA) and imaged on a 510 confocal laser scanning microscope (Carl Zeiss MicroImaging, Thornwood, NY). Images were analyzed in MATLAB by fitting an ellipse to each nucleus and calculating the orientation of the major axis relative to the expected angle.

### 2.2.6 Statistical Analysis

All data were expressed as mean ± standard error of the mean. Rayleigh's test of uniformity and all other statistics for phase shift data were performed using the Circular Statistics Toolbox for Matlab. The variances of phase shift were compared using an F-test. Mechanical data were analyzed with a 2 factor ANOVA, while fiber alignment data were analyzed with a one-way ANOVA. Fisher's post-hoc test was used for all ANOVA data. Significance was reported at the 95% confidence interval ($\alpha$=0.05).

## *2.3 Results*

### 2.3.1 Gross Morphology of Electrospun PCL Scaffolds

The scaffolds produced by the masked electrospinning process were affected by the shape of the aperture in the insulating mask used for their production (Figure 4).

The square mask produced circular scaffolds with edges just touching all four sides of the mask, while the rectangular mask produced scaffolds that were elliptical, touched only the two long sides of the mask, and had only a few fibers that were deposited directly on the mask. The scaffolds were otherwise similar in gross morphology and appeared similar by scanning electron microscope (Figure 5). The mean thickness of the scaffolds used for mechanical testing was 0.35 ± 0.02 mm for the aligned scaffolds and 0.30 ± 0.02 mm for the unaligned scaffolds ($p = 0.11$).

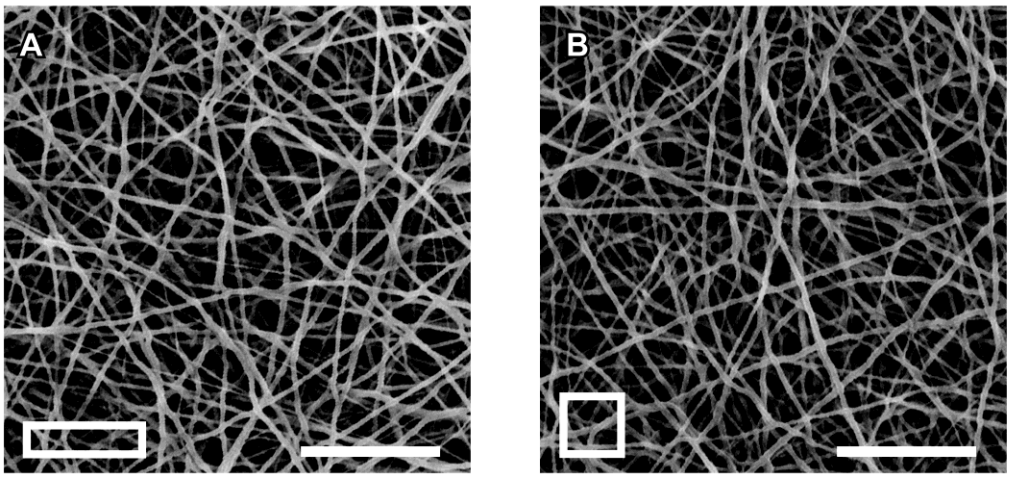


**Figure 5: Scanning Electron Micrographs of scaffolds produced using (A) Rectangular Mask (Aligned scaffold) and (B) Square Mask (Unaligned scaffold). Expected axis is horizontal. (1000x magnification. Scale bar = 50 μm.)**

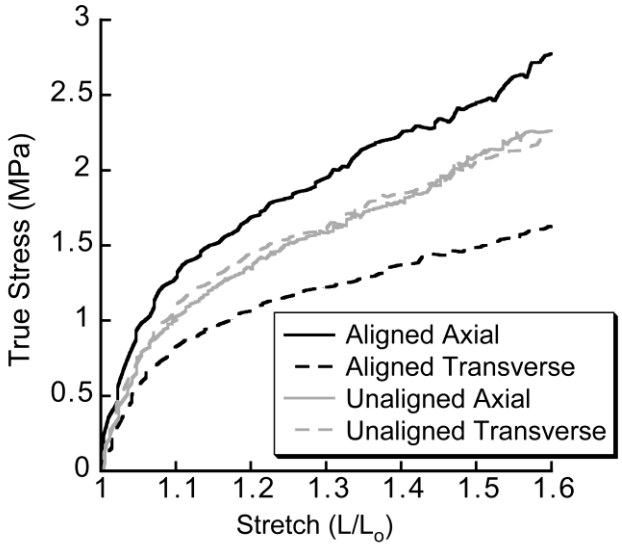


**Figure 6: True stress v. stretch curves for representative scaffolds. Note that the axial and transverse unaligned curves are almost superimposed and the aligned scaffolds show higher stress and stiffness in the axial direction compared to the transverse direction.**

### 2.3.2 Tensile Testing

Aligned scaffolds (produced using a rectangular mask) displayed distinct mechanical anisotropy, while the unaligned scaffolds (produced using a square mask) did not (Figure 7). The aligned scaffolds were stiffer in the axial direction than the transverse direction at 0 strain (22.9 ± 1.3 MPa axial, 16.1 ± 0.9 MPa transverse; $p < 0.0005$), and at 0.1 strain (4.8 ± 0.3 MPa axial, 3.5 ± 0.2 MPa transverse; $p < 0.001$) ($n = 12, 13$). The unaligned scaffolds did not show this difference, with similar stiffness in the axial and transverse directions at 0 strain (19.7 ± 1.4 MPa axial, 20.8 ± 1.3 MPa transverse; $p = 0.54$) and 0.1 strain (4.4 ± 0.2 MPa axial, 4.6 ± 0.3 MPa, transverse; $p = 0.70$) ($n = 11$ per group). The scaffolds displayed a strain-softening or yielding response characterized by

linear regions at 0 strain, decaying to a lower modulus linear region at high strain (Figure 6).

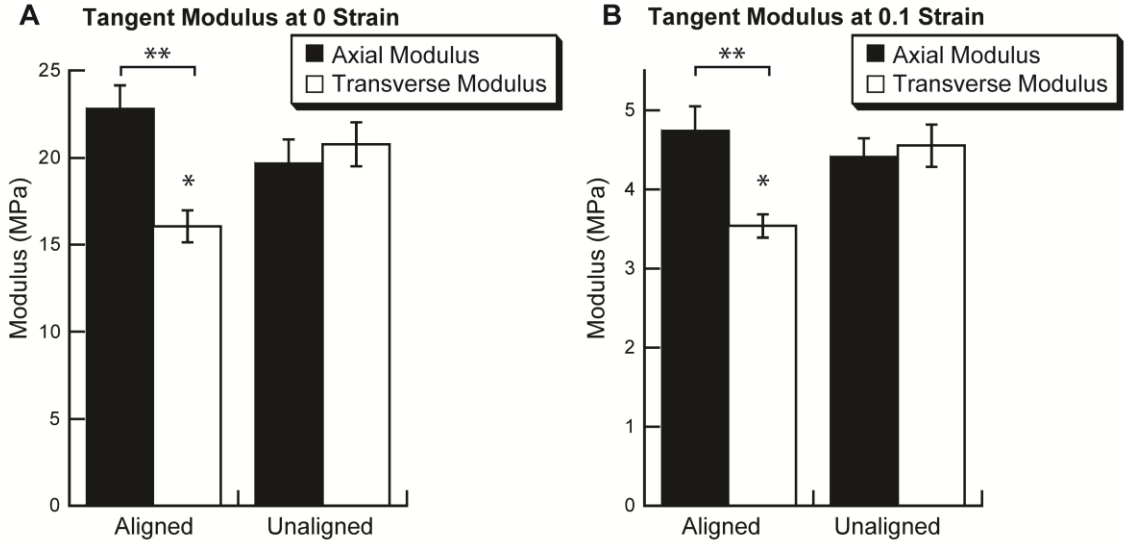


**Figure 7: Tangent Moduli at (A) 0 strain. (B) 0.1 strain for scaffolds tested in axial and transverse directions. Aligned scaffold, axial and transverse directions different at $p < 0.0005$ for 0 strain, $p<0.001$ for 0.1 strain. Unaligned scaffold, axial and transverse directions not different: $p = 0.54$ for 0 strain, $p = 0.70$ for 0.1 strain. (Mean±SEM) * Denotes that aligned transverse modulus is different from all other groups, $p<0.05$.**

### 2.3.3 Fiber Alignment

The aligned scaffolds exhibited a higher Fiber Alignment Index (0.97 ± 0.16) than the unaligned scaffolds, where it approximated 0 (0.11 ± 0.15) ($p < 0.0005$) (Figure 8A,B). Aligned scaffolds showed a trend towards exhibiting better fits to a sine curve ($R^2 = 0.52 \pm 0.09$) than the unaligned scaffolds ($R^2 = 0.30 \pm 0.09$) ($p = 0.076$). Aligned scaffolds also showed greater amplitude (0.73 ± 0.15) than the unaligned scaffolds (0.42 ± 0.12) ($p = 0.087$) (Figure 8C), and smaller phase shifts (0.26 ± 0.16 rad vs. 1.08 ± 0.42 rad for

unaligned) with a much smaller range ($p < 0.05$) and higher mean vector magnitude (0.88 vs. 0.29 for unaligned) (Figure 8D). The phase shift values fit a von Mises distribution for the aligned scaffolds, ($p < 0.0005$), but not for the unaligned scaffolds ($p = 0.53$).

### 2.3.4 Multilayer Fiber Alignment

Multilayered scaffolds showed more alignment in the top layer (Fiber Alignment Index: $1.98 \pm 0.16$) than single-layered aligned scaffolds ($p < 0.0001$) (Figure 8B). The sine curves showed higher amplitude ($1.69 \pm 0.07$) than the single layered aligned scaffolds ($0.73 \pm 0.15$, $p < 0.0001$). The top layer of the multilayered scaffolds showed phase shift of $0.01 \pm 0.13$ with a mean vector magnitude of 0.96, and conformed to a von Mises distribution ($p < 0.001$).

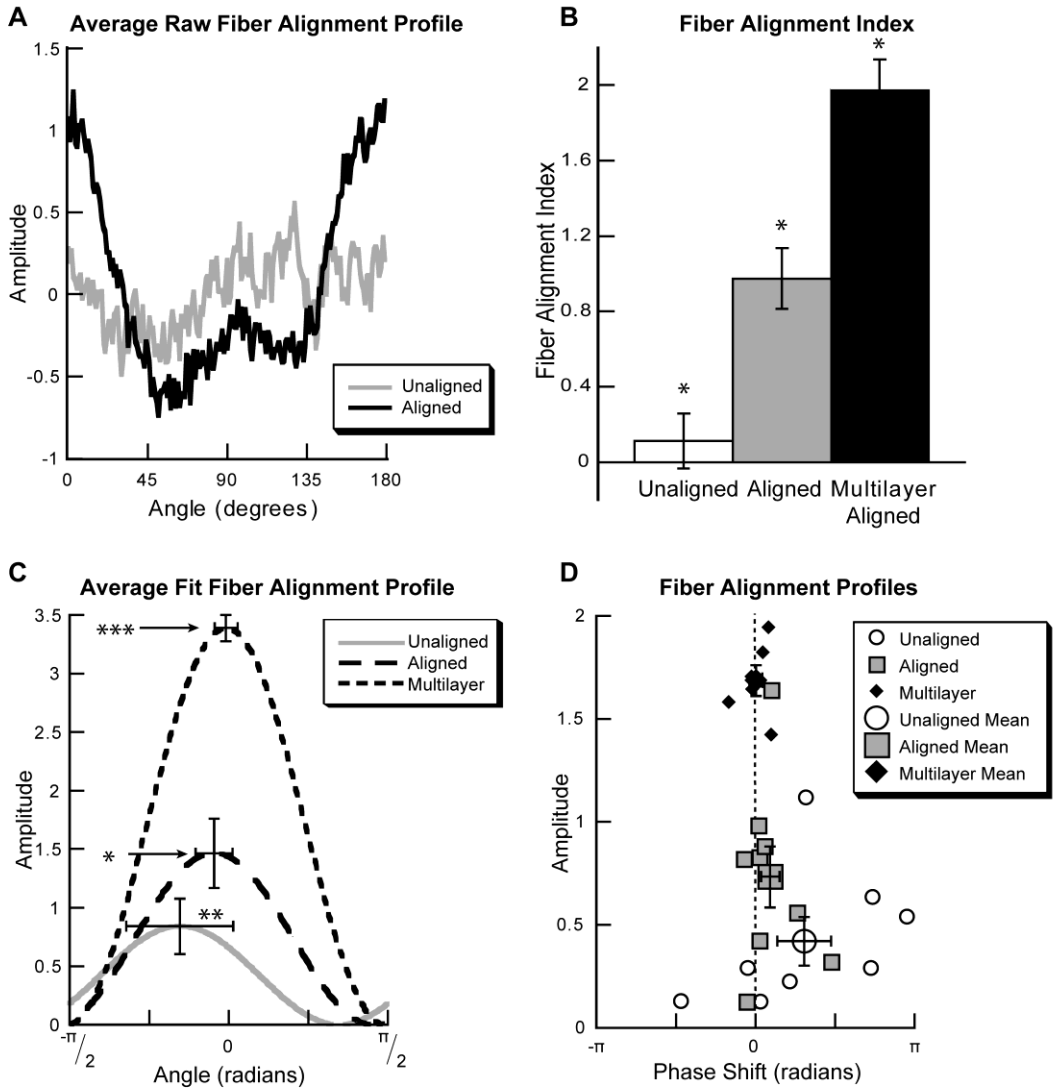


**Figure 8: Fiber Alignment. (A) Average fast Fourier Transform profiles of Aligned and Unaligned scaffolds (n=8-9 scaffolds per group). (B) Fiber Alignment Index for unaligned, aligned, and multilayer aligned scaffolds. All groups are different ($p<0.0005$). (Mean±SEM) (C) Sine curve constructed from mean fit parameters, showing SEM of amplitude and phase shift. * amplitude of aligned greater than amplitude of unaligned ($p=0.087$). *** amplitude of multilayer aligned greater than other groups ($p<0.00001$). ** variance of unaligned phase shift greater than other groups ($p<0.05$). (D) Fiber alignment profiles for each unaligned, aligned and multilayer aligned scaffold, and means for each group. Note distribution of aligned and multilayer aligned scaffolds near 0 phase shift and distribution of unaligned scaffold over a much greater phase shift range.**

### 2.3.5 Cell Alignment

Nearly all of the cells cultured on the single layer scaffolds had an elliptical nucleus (scaffolds had 92.7 ± 0.5% of nuclei with an aspect ratio greater than 1.5), and most scaffolds had a principal direction of cell alignment, with more cells being oriented in one direction (Figure 9). The aligned scaffolds showed a greater degree of cell alignment than the unaligned scaffolds, with more cells oriented close to the principal direction of alignment (standard deviation 0.288 ± 0.018 rad, compared to 0.496 ± 0.029, $p < 0.0005$), and a larger mean vector magnitude (0.83 ± 0.02, compared to 0.50 ± 0.06, $p < 0.0005$). The cell orientation in the aligned scaffolds was close to the expected axis (0.015 ± 0.056 rad), while in the unaligned scaffolds, it was not (1.005 ± 0.225 rad) (different at $p < 0.05$). Additionally, the principal direction of alignment for each scaffold varied less for the aligned scaffolds than the unaligned scaffolds ($p < 0.01$).

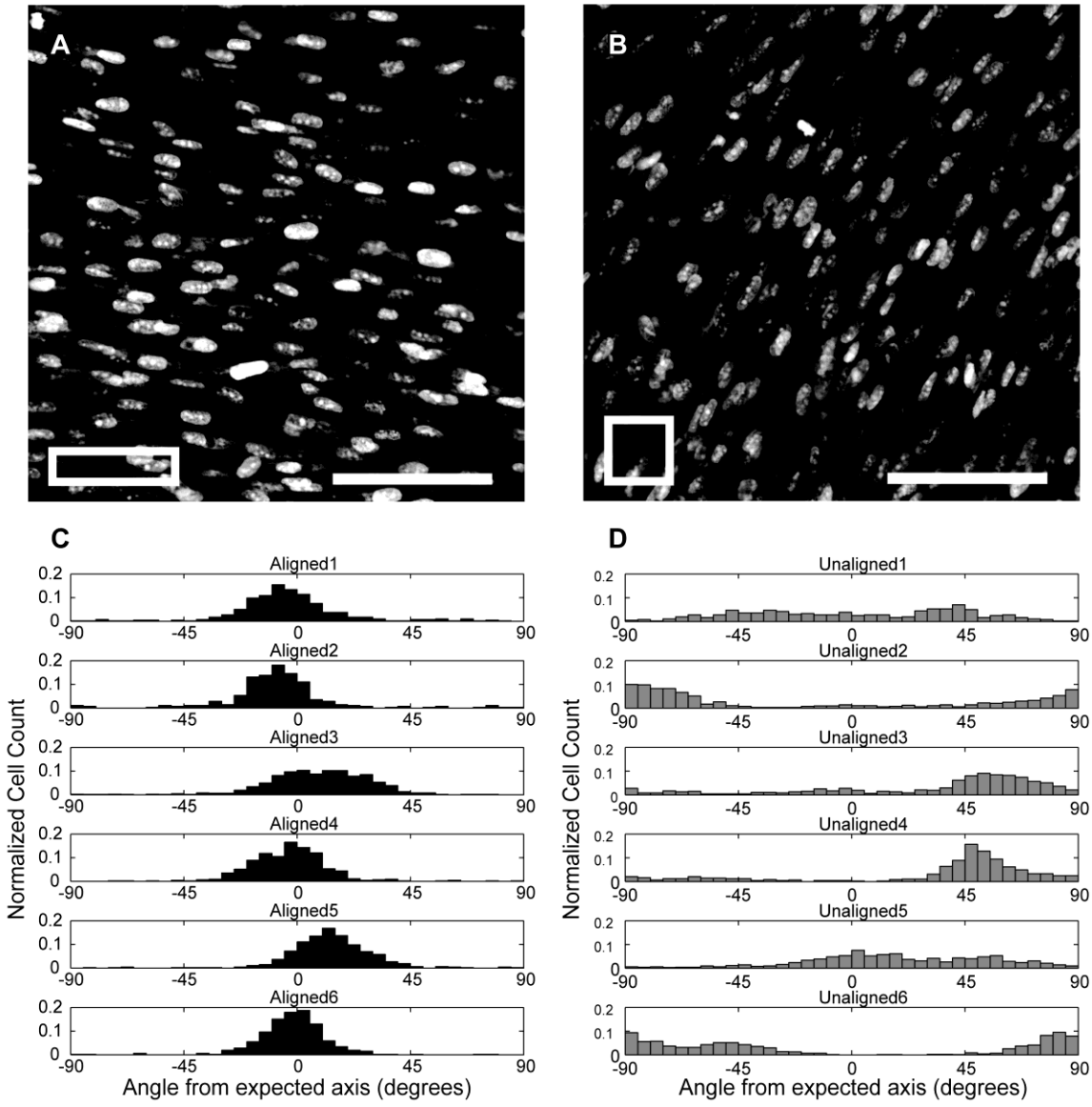


**Figure 9: Syto13 stained adipose stem cell nuclei cultured on (A) aligned and (B) unaligned scaffolds. Expected axis is horizontal. Scale bar = 100 μm. (C, D) Cell orientation histograms from 6 (C) aligned and (D) unaligned scaffolds.**

## *2.4 Discussion*

Our findings present a novel method for creating a multilayered electrospun scaffold, with each layer having its own preferred direction of fiber alignment in order

to mimic human tissues. The results of this study demonstrate that macroscopic shaped insulating masks can be used to create aligned multilayered scaffolds with each layer having anisotropy in a different direction. Mechanical anisotropy with approximately 30-40% difference in stiffness is associated with increased fiber alignment, and alignment of adipose stem cells cultured on the surface.

Scaffolds produced using a rectangular insulating mask showed a significant difference of approximately 35% in tensile moduli in two orthogonal directions. Such anisotropy primarily has been achieved in the past using rapidly spinning mandrels, physically pulling the fibers into alignment.(Nerurkar, Baker et al. 2006; Baker and Mauck 2007; Nerurkar, Elliott et al. 2007; Carnell, Siochi et al. 2008; Baker, Nathan et al. 2009) This spinning mandrel method can produce much higher levels of anisotropy, which can exceed modulus ratios of 10:1 at high spinning rates.(Li, Mauck et al. 2007) The approach described here introduces lower levels of anisotropy (approximately 35% difference in moduli), but which are similar to those observed in native tissues. For example, native articular cartilage possesses a similar level of anisotropy as the scaffolds produced with our method described here. The cartilage of the humeral head has a tensile modulus of 7.8 MPa in the direction of the split lines, and 5.9 MPa perpendicular to them. This difference of 32-35% stiffer in the split line direction is maintained throughout the thickness of the cartilage and increased to 63% in the surface zone at 0.16 strain.(Huang, Stankiewicz et al. 1999) The aligned scaffolds presented here are 42%

stiffer in the axial direction at 0 strain and 34% stiffer at 0.1 strain, which is similar to published values for cartilage.(Verteramo and Seedhorn 2004) Though the level of anisotropy of the produced scaffolds is lower than in those made with a spinning mandrel, the technique described here achieved a comparable level of anisotropy to cartilage, while allowing multiple directions of alignment in subsequent layers. Increasing the aspect ratio or otherwise changing the shape of the insulating mask could provide further anisotropy in the resulting scaffolds. Furthermore, the process described may be particularly useful for the engineering of tissues that display inhomogeneity in the mechanical anisotropy with different layers, such as the anulus fibrosus, which has successive layers with principal orientations 30° on either side of the spine's transverse axis.(Nerurkar, Baker et al. 2009)

The introduction of anisotropy to the scaffolds using the described technique occurs through the increased alignment of fibers in a preferred direction, similar to what has been reported with other anisotropic electrospinning methods.(Ayres, Bowlin et al. 2006; Ayres, Bowlin et al. 2007; Li, Mauck et al. 2007; Ayres, Jha et al. 2008) This directionality is relatively subtle and not noticeable by simple observation (Figure 5). The Fiber Alignment Index reported here provides a means of simplifying the FFT data into a single quantity (Figure 8B). A positive value of the index indicates that a group of scaffolds shows alignment along the expected direction, as in the aligned scaffolds (0.97 ± 0.16). Because it represents the magnitude of the profile in the preferred direction after

the profile has been centered on 0, a group of scaffolds without a preferred direction has an expected value of 0, as we see with the unaligned scaffolds ($0.11 \pm 0.15$). However, the profiles from unaligned scaffolds often display some degree of periodicity, and averaging them together can obscure this. Therefore, we further investigated how these scaffolds appear to display fiber alignment when examined individually.

Amplitude and phase shift values are more instructive than the Fiber Alignment Index in understanding the fiber alignment in individual electrospun scaffolds (Figure 8C,D). Though the amplitude was higher in the aligned scaffolds than in the unaligned scaffolds, as expected, the amplitude in the unaligned scaffolds was not zero, showing that the unaligned scaffolds show some degree of periodicity in their profiles. The phase shifts, which give the preferred alignment angle, were grouped near the expected alignment value of 0 for the aligned scaffolds, but were distributed uniformly across the full possible range in the unaligned scaffolds (Figure 8D). Examining the mean for each type of scaffold demonstrates that the profiles of the unaligned scaffolds are not flat, but do show a large variation in phase shift. This variation in phase shifts in the unaligned scaffolds results in a flat line when scaffolds from an entire group are averaged together (Figure 8A). On the other hand, the aligned scaffolds have a much narrower range of phase shifts, causing the averaging of an entire group to preserve the periodic shape. This explains why the Fiber Alignment Index is near 0 for the unaligned scaffolds, but each scaffold does show periodicity. This analysis provides insights into how fibers are

aligned in electrospun scaffolds. We have demonstrated that electrospun scaffolds exhibiting mechanical isotropy tend to show surface fiber alignment in an arbitrary direction. The fiber orientation in the aligned scaffold was consistent with the alignment of the long sides of the rectangular insulating mask.

Fiber alignment occurs based on the orientation of attractive forces generated by the shaped collector electrode. Previous work has shown that fibers collected on a thin electrode surrounded by insulators show orientation along the axis of the electrode.(Li, Ouyang et al. 2005) Our results indicate that this effect persists when the elongated electrode is widened from less than 1 mm to 2.5 cm. The technique described here allows this alignment due to an elongated electrode to be harnessed for use in a multilayered scaffold.

The multilayer scaffolds exhibited more pronounced alignment in the top layer than the single-layer scaffolds. Because the bottom layer was manufactured in an identical way to the single layered scaffolds, this data indicates that anisotropy can be imparted by the rectangular mask even if the collector electrode is partially covered by a previous layer. Further, this partial coverage of the collector electrode is most likely the cause of the increased fiber alignment in the top layer. As the second layer is deposited, the central area is concealed by the previous layer, forming an insulator between two exposed electrodes. An insulator between electrodes has been shown to align the fibers between the electrodes.(Li, Wang et al. 2003; Li, Wang et al. 2004)

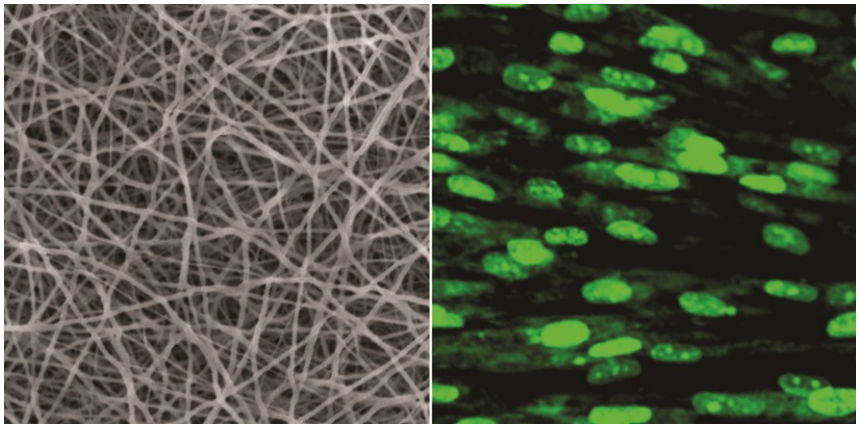

**Figure 10: (A) Scaffold and (B) adipose stem cell nuclei cultured on aligned scaffold. Note the alignment of the cells despite the lack of subtlety of fiber alignment.**

The differences between aligned and unaligned scaffolds were also observed in the cell alignment studies (Figure 9). Cells seeded on the scaffold surfaces exhibited local regions of alignment, as measured by the principal direction of the nuclei, in both aligned and unaligned scaffolds. Aligned scaffolds showed a significant mean cell orientation in the principal axis of alignment of the scaffold, whereas unaligned scaffolds showed a smaller but nonzero level of cell alignment in random directions.

In summary, this study provides proof-of-concept of a novel method for creating multilayered anisotropic electrospun scaffolds for tissue engineering that may meet the mechanical needs of tissue as well as influence the alignment of cultured cells. The use of a rectangular insulating mask induces a preferential alignment direction into scaffolds. Cells seeded onto these scaffolds also showed preferential alignment along the expected axis of alignment of the insulating mask. Further studies are needed to

examine the growth and differentiation of cells on these scaffolds as well as the influence of alignment on the long-term mechanical properties of cell-seeded constructs.

# 3. Electrospun multilayered and cartilage-derived matrix scaffolds

## *3.1 Introduction*

The repair or regeneration of injured or diseased tissues through tissue engineering often focuses on biomaterial scaffolds, cells, and bioactive molecules to create new tissues. Musculoskeletal tissues and other tissues that serve a primarily biomechanical role face a unique set of challenges.(Butler, Goldstein et al. 2000) Articular cartilage, with its sparse cell population, has its mechanical properties chiefly determined by the extracellular matrix. Therefore, the location, type, and quality of extracellular matrix proteins play a vital role in providing and maintaining the appropriate mechanical properties.(Kempson, Muir et al. 1973; Mow, Kuei et al. 1980; Huang, Stankiewicz et al. 1999; Mow and Guo 2002; Ateshian and Hung 2003; Mow and Huiskes 2005) It is imperative for a tissue-engineered scaffold to allow cells to infiltrate throughout the scaffold in order to deposit locally homogeneous extracellular matrix, as well as encouraging them to produce the proteins required for tissue growth and maintenance.

Electrospun scaffolds have been used in the engineering of various tissues, ranging from cartilage, bone, and tendon, to blood vessel, nerve, and heart valve.(Little, Guilak et al.; Li, Laurencin et al. 2002; Li, Danielson et al. 2003; Yoshimoto, Shin et al. 2003; Boland, Matthews et al. 2004; Shin, Yoshimoto et al. 2004; Li, Tuli et al. 2005; Yang, Murugan et al. 2005; Courtney, Sacks et al. 2006; Li, Vepari et al. 2006; Li, Jiang et al.

2006; Baker and Mauck 2007; Chew, Mi et al. 2008; Kumbar, Nukavarapu et al. 2008; Baker, Nathan et al. 2009) The flexibility of the electrospinning process allows the production of fibers of various materials, chemically functionalized fibers, drug-eluting fibers, aligned fibers, and scaffolds with controllable mechanical anisotropy.(Li, Wang et al. 2003; Li, Wang et al. 2004; Chew, Wen et al. 2005; Li, McCann et al. 2005; Li, Ouyang et al. 2005; Buttafoco, Kolkman et al. 2006; Mauney, Nguyen et al. 2007; Garrigues, Little et al. 2010) The nanoscale fiber diameter encourages chondrocytes to maintain their phenotype when they are cultured on electrospun scaffolds, and improves *in vivo* toleration of fibrous scaffolds.(Sanders, Stiles et al. 2000; Li, Danielson et al. 2003; Sanders, Cassisi et al. 2003; Li, Jiang et al. 2006)

### 3.1.1 Materials for Electrospinning

When using an electrospun scaffold for tissue engineering, synthetic polymers are commonly used.(Li, Mauck et al. 2005) This can mean custom polymers that have been specifically functionalized or FDA-approved materials which are well known to be biocompatible.(Li, Laurencin et al. 2002; Li, Danielson et al. 2003; Casper, Yamaguchi et al. 2005; Li, McCann et al. 2005) These synthetic polymers can be selected based on features such as degradation rate, stiffness, and cellular adhesion, but cannot provide the same cell-matrix interactions which cells would receive in their native environment. This has led to the electrospinning of purified proteins such as collagen, elastin, and silk.(Matthews, Wnek et al. 2002; Boland, Matthews et al. 2004; Shields, Beckman et al.

2004; Zhong, Teo et al. 2005; Zhong, Teo et al. 2007) However, purified proteins may have different conformations than native proteins, and in the case of many tissues, there are proteins present in the tissue, such as bioactive molecules, which are impossible to retain throughout the purification process. Platelet-rich plasma and small intestine submucosa have been incorporated into electrospun scaffolds.(Hong and Kim 2010; Hong and Kim 2010; Sell, Wolfe et al. 2011) Scaffolds derived directly from cartilage (cartilage-derived matrix, or CDM) has been shown to induce cartilage-specific gene expression in adipose stem cells, indicating that using native proteins within a tissue engineering scaffold is a useful strategy.(Cheng, Estes et al. 2009) Therefore, we undertook to use native, unpurified tissue, and incorporate it into electrospun scaffolds for tissue engineering.

### 3.1.2 Scaffold Structure

In order to engineer a tissue that can maintain and remodel itself, cells must be able to infiltrate throughout the entire thickness of the scaffold to allow deposition of extracellular matrix throughout the thickness of the engineered tissue. This has proven difficult to accomplish with electrospun scaffolds due to the small pore sizes which result from narrow fibers.(Eichhorn and Sampson 2005) Previous attempts to improve cellular ingrowth have included the centrifugation of loose fibers and cells together(Li, Jiang et al. 2008) or using differential fiber sizes or soluble placeholders to control pore size.(Pham, Sharma et al. 2006; Nam, Huang et al. 2007; Kim, Chung et al. 2008) Most

electrospun scaffolds for tissue engineering show little cellular infiltration, and the majority of protein accumulation occurs near the surface of the scaffold in the form of overgrowth. However, collecting multiple layers of electrospun scaffolds on a water bath, followed by vacuum expansion created a scaffold that allowed for superior cellular infiltration.(Tzezana, Zussman et al. 2008) Therefore, we used a similar, layered approach to cartilage tissue engineering.

### 3.1.3 Experiment

In this study, we developed a method for making electrospun scaffolds which incorporate cartilage tissue in order to improve cellular response, and saw evidence that these scaffolds had a chondrogenic effect. Moreover, we showed that vacuum expansion of layered electrospun scaffolds is not necessary to vastly improve the migration of cells into the interior of a scaffold and the deposition of extracellular matrix there. We analyzed the structure of the scaffolds over their time in culture, as well as gene expression and protein content of the scaffolds when cultured with adipose stem cells.

## *3.2 Materials and Methods*

### 3.2.1 Cartilage-Derived Matrix production

Articular cartilage was harvested in large slices from the femoral condyles and trochlear groove of 2-3 year old skeletally mature female pigs obtained from a local abattoir. The cartilage was frozen at -80 °C overnight, lyophilized, and crushed until

the flakes measured roughly 5 mm, before being repeatedly pulverized to a fine powder using a freezer mill. Several batches of cartilage-derived matrix (CDM) were pooled to a single source for the described experiments.

### 3.2.2 Electrospinning

CDM powder was dissolved at 0.08 g/ml in Hexafluoroisopropanol for 24 hours before being filtered twice through 84 mesh (0.18 mm pores). Polycaprolactone ($M_n$ = 80,000) was added at 0.08 g/ml and dissolved for 24 hours to prepare CDM solution for electrospinning. This CDM solution was pumped at 1.2 ml/hr through a 21 gauge needle fitted with a round focusing cage (3 cm diameter, needle tip protrudes 4 MM). The electrospun fibers were collected on the surface of a grounded saline solution (NaCl 1.25 g/l in distilled water) 20 cm away. The applied voltage was 25 kV. (These scaffolds will be referred to as "CDM scaffolds.") For multilayered scaffolds, 60 layers were collected on a large glass slide at 1 minute intervals, with minimal liquid draining between layers. Single-layer scaffolds were collected for 60 minutes.

PCL scaffolds were prepared similarly to CDM scaffolds. PCL was dissolved overnight at 0.1 g/ml in 70% Dichloromethane and 30% Ethanol. This solution was pumped at 1.2 ml/hr through a 25 gauge needle with a round focusing cage into the saline bath 20 cm away. The applied voltage was 17 kV. Multilayered scaffolds consisted of 60 layers collected at 1 minute intervals with minimal liquid draining.

Single-layered scaffolds were collected for 180 minutes to ensure comparable scaffold thickness.

Immediately after collection, scaffolds were frozen at -80°C overnight, followed by lyophilization.

### 3.2.3 Fiber characterization

Scaffolds were visualized using a scanning electron microscope (SEM) (FEI XL30 ESEM, Hillsboro, OR) after sputter coating with gold and palladium (DeskIV, Denton Vacuum, Moorestown, NJ). These images were used to measure the diameter of 183-190 individual fibers from each scaffold type ImageJ(Rasband 1997-2011).

### 3.2.4 Experimental layout

Four types of scaffolds were manufactured according to the factors of material (CDM vs. PCL) and structure (60-layer vs. 1-layer). These scaffolds were seeded with human adipose stem cells (or left acellular in the case of controls) and cultured for up to 28 days before being analyzed for gene expression, biochemical composition, microstructure, and mechanical properties.

### 3.2.5 Cell seeding and culture

Scaffolds were cut into 8 mm diameter discs for tissue culture and distributed evenly among the groups. Sterilization was conducted by soaking in 70% ethanol and irradiating with ultraviolet light for 10 minutes on each side. Ethanol was removed and

replaced with phosphate buffered saline. After 5 more minutes of ultraviolet irradiation, the samples were incubated for 18 hours at 37 °C.

Human adipose stem cells from 3 donors were expanded to passage 4 and seeded in expansion medium consisting of DMEM/Hams F-12 with 15 mM HEPES, L-glutamine, and pyroxidine hydrochloride (Lonza), supplemented with 10% fetal bovine serum (Atlas), 1% ITS+, 5 ng/ml recombinant human epidermal growth factor, 1 ng/ml recombinant human basic fibroblastic growth factor, 0.25 ng/ml TGF-β1, and 1% penicillin/streptomycin/fungizone.

500,000 human adipose stem cells, pooled from 3 donors at passage 4, were seeded on each scaffold at seeding density of 1 million cells/cm$^2$. Half of the cells were suspended in 50 μl of expansion medium seeded on one side and given one hour to attach before repeating on the other side. After another 1 hour incubation, 1 ml of chondrogenic medium was carefully added.[1] Day 0 scaffolds were harvested after 1 hour in the full media volume.

Seeded scaffolds were grown in low-attachment tissue culture plates with chondrogenic medium consisting of DMEM-high glucose (Gibco), 10% fetal bovine serum (Atlas), 1% penicillin/streptomycin (Gibco), 1% ITS+, 100nM dexamethasone, 37.5 μg/ml ascorbate, 40 μg/ml proline, 10 ng/ml bone morphogenic protein-6 (BMP-6), and

[1] With the exception of samples for gene expression analysis, day 0 samples were feed with 1 ml of expansion medium, rather than chondrogenic medium.

10 ng/ml transforming growth factor β1 (TGF- β1). This chondrogenic medium was changed every 2 days.

Acellular scaffolds were cultured in a simple medium of DMEM-high glucose, 10% fetal bovine serum, and 1% penicillin/streptomycin.

### 3.2.6 Biochemical analysis

In order to partially characterize the biochemical composition of the cultured constructs, 6 constructs from each group were lyophilized and digested with papain (125 μg/ml) at 60°C for 15 hours for analysis of specific biochemical components. Sulfated glycosaminoglycans were measured using the dimethylmethylene blue assay , total collagens using the hydroxyproline assay and normalized to dry weight. All values that were calculated negative were corrected to 0. Double-stranded DNA was quantified with the PicoGreen assay (Quant-IT kit, Invitrogen).

### 3.2.7 Gene expression analysis

Gene expression was analyzed on cell-seeded scaffolds over the course of the first 2 weeks of culture. 3 constructs from each scaffold type were harvested at 0, 1, 3, 7, and 14 day time points, as well as cells at day 0 which had not been seeded onto a scaffold. The constructs were snap-frozen in liquid nitrogen and stored at -80 °C for up to 3 days before being individually pulverized in a freezer/mill (SPEX Sample Prep) (3 minutes precool, 2 minutes run, 2 minutes cool between cycles, 5 Hz, for 3 cycles). The pulverization tubes were rinsed repeatedly with 0.6 ml of RLT buffer supplemented

with 0.1% 2-mercaptoethanol to recover all residue from the construct, before freezing at -80 °C. The pulverized tissue lysate was homogenized (QIAshredder, Qiagen, Valencia, CA), and the RNA isolated and stabilized (RNeasy mini kit, Qiagen), before reverse transcription (SuperScript VILO cDNA synthesis kit, Invitrogen, Carlsbad, CA). Real-time PCR was for extracellular matrix proteins aggrecan (ACAN) and collagen II (COL2A1) (positive markers of chondrogenesis), collagens I (COL1A1) and X (COL10A1)(negative markers of chondrogenesis), as well as 18S rRNA (reference gene). Data were analyzed according to the comparative $C_T$ method, corrected for efficiency, and normalized to 18S.(Pfaffl 2001) Data are reported as fold-change relative to the gene expression in a sample of the same population of cells harvested at day 0 that were not seeded on scaffolds.

### 3.2.8 Histology and immunohistochemistry

Cultured constructs were embedded in OCT upon harvest and 8 μm thick sections were taken with a cryotome. These sections were stained with Safranin-O, Fast Green, and Hematoxylin to visualize proteoglycans, collagens, and cell nuclei, respectively. Additionally, sections were analyzed for collagen II content using immunohistochemistry with a mouse monoclonal antibody (U. of Iowa), goat anti-mouse secondary (Abcam), and an immunohistochemistry kit (Invitrogen) which used a DAB/HRP system for chromagen development.

### 3.2.9 Statistical analysis

All data were analyzed by ANOVA, followed by Fisher's Least Significant Difference post-hoc test in cases where the main effect had $p < 0.05$. Biochemical data was analyzed by an ANOVA of all data at day 0, as well as separate ANOVAs of all data split into cell-seeded and acellular groups.

## *3.3 Results*

### 3.3.1 Scaffold appearance and structure

All four types of scaffolds had similar thickness (main effects $p > 0.29$) (Figure 11). The PCL scaffolds were smooth, and exhibited very little macroscale texture, as the fibers were quite homogeneous. Multilayered scaffolds were quite soft, due to the void space between the layers and the fact that the layers could move freely relative to each other. CDM scaffolds had some fragments of undissolved cartilage which disrupted the smooth texture. In the multilayered CDM scaffolds, these fragments did not have a noticeable effect on the overall scaffold appearance, while the resulted in a grainy structure in the single-layered CDM.

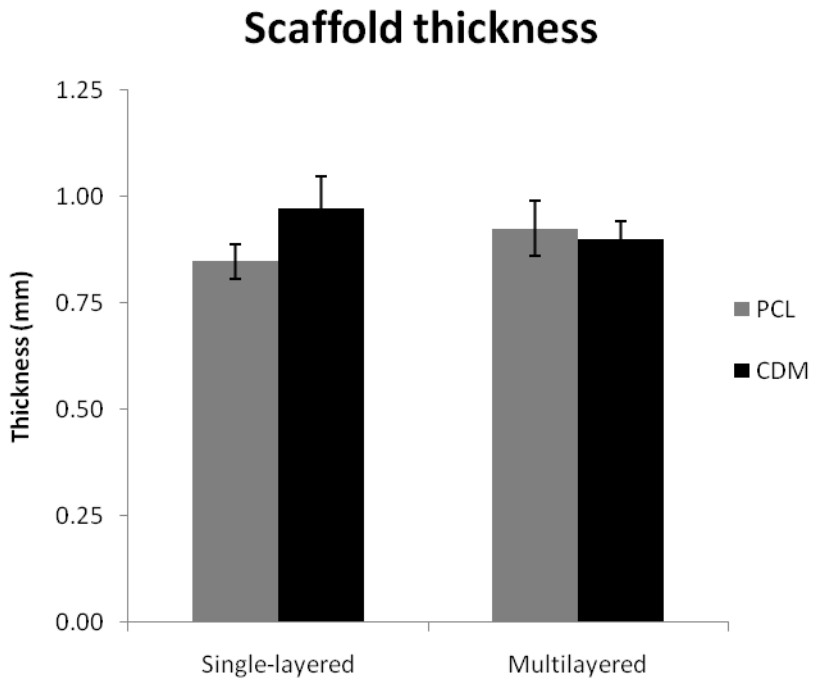


**Figure 11: Scaffold thickness. All scaffolds have 60 minutes of electrospun layers, except 1L PCL, which has 180 minutes to attain a comparable thickness. Scaffolds did not show any difference in thickness ($p>0.29$ for main effects.)**

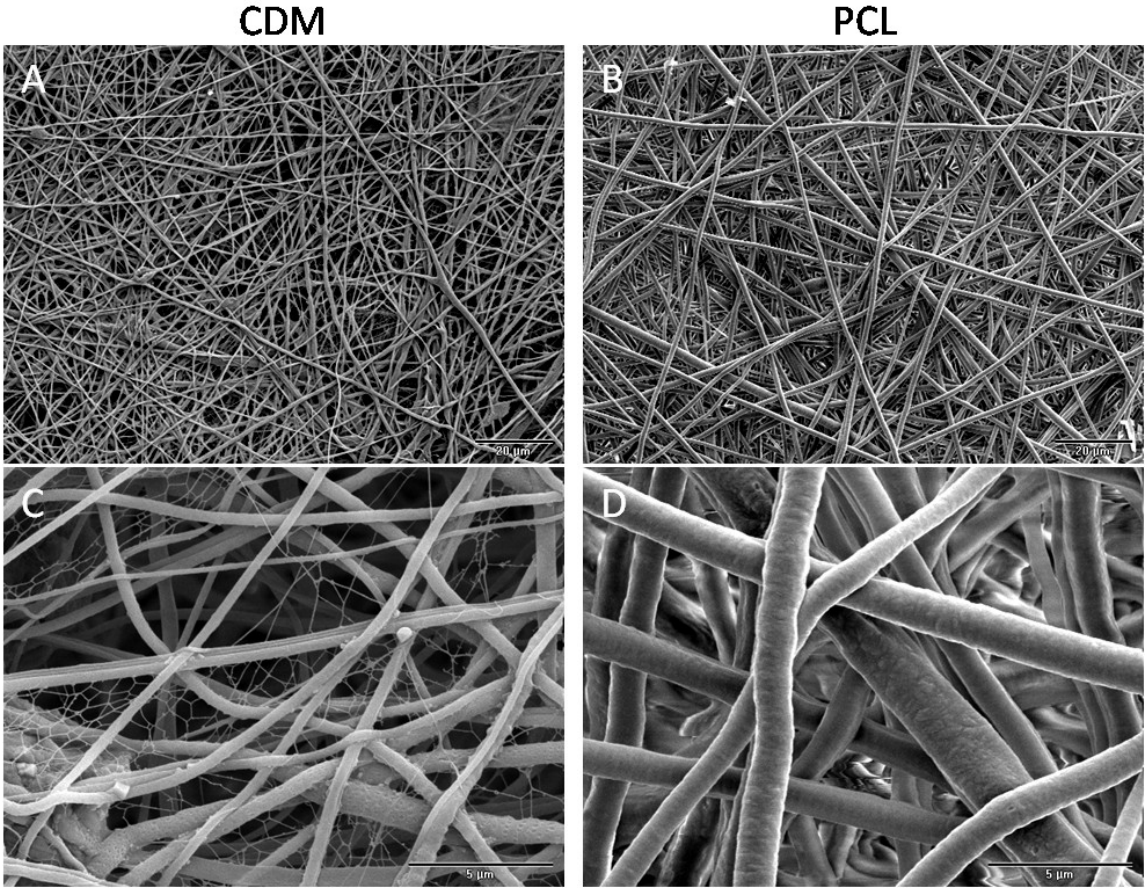


**Figure 12: Scanning electron microscope images of electrospun scaffolds. (A,C) CDM scaffolds. (B,D) PCL scaffolds. The fibers are quite similar in appearance between the two materials, though the CDM scaffolds have smaller fibers, as well as a network of extremely fine fibers in some areas. Scale bars in A, B are 20 μm, scale bars in C, D are 5 μm. All images are from single-layered scaffolds.)**

### 3.3.2 Fiber size and shape

The scaffolds surface of the scaffold, as viewed by SEM (Figure 12), had smooth fibers with few loops, beads, or fragments. Fiber thickness in CDM scaffolds was not different between single-layered (0.58 ± 0.02 μm diameter) and multilayered (0.56 ± 0.01 μm) ($p = 0.60$), but was smaller than in PCL scaffolds ($p < 0.0001$). Single-layered PCL had smaller diameter fibers (1.40 ± 0.03 μm) than multilayered PCL (2.21 ± 0.04 μm) ($p < 0.0001$). Both types of scaffold appeared to have small populations of fibers with smaller diameters than the rest (Figure 13). PCL scaffolds appeared to have an additional population of fibers with 0.9 μm diameter., while CDM scaffolds had fibers with a mean diameter of 50 nm, which were too small and sparse to adequately measure the frequency (visible in Figure 12) that appeared to be originating from flattened extensions along the sides of the thicker fibers. These extremely small fibers present in the CDM scaffold are present as a network of fibers that are bound to each other.

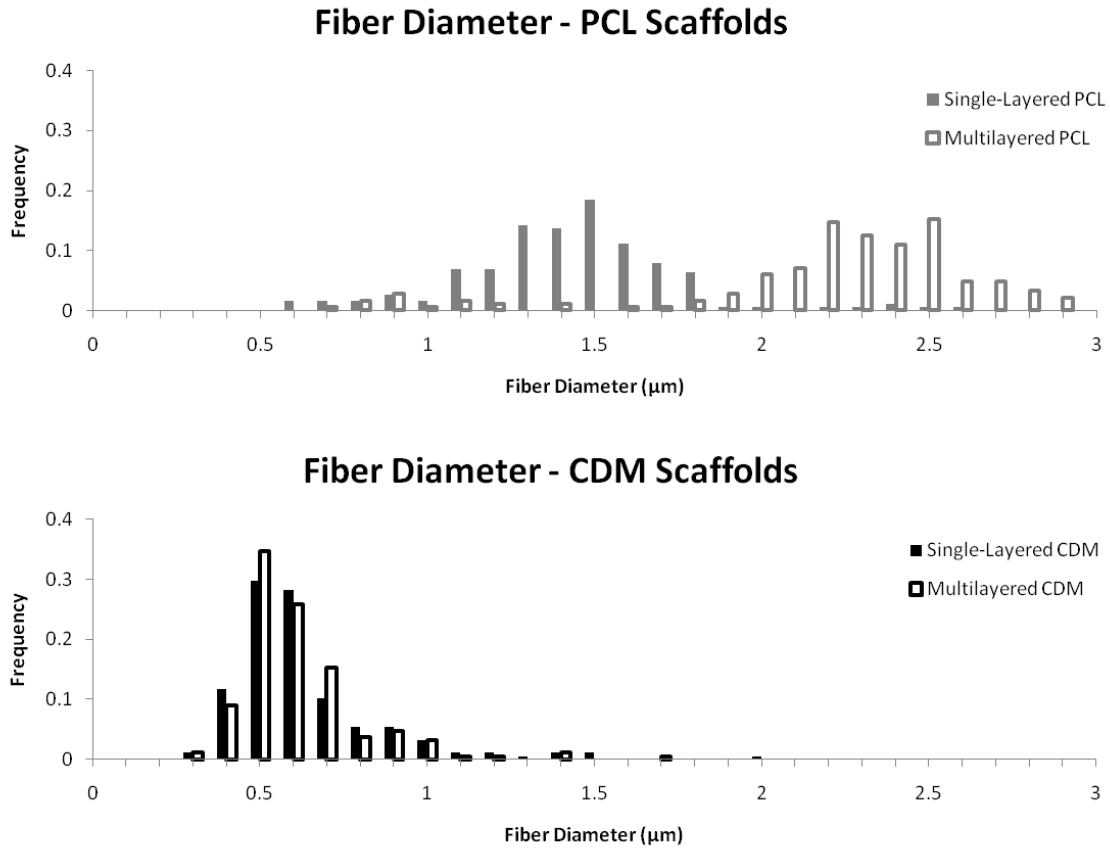


**Figure 13: Fiber diameter. (A) Multilayered PCL scaffolds have thicker fibers than single-layered PCL scaffolds. ($p<0.0001$) (B) CDM scaffolds had smaller fibers than PCL scaffolds ($p<0.0001$), but fiber diameter did not vary between single-layered and multilayered CDM ($p=0.6$).**

### 3.3.3 Histology and Immunohistochemistry

Histological sections of acellular PCL scaffolds showed that they did not have any collagen or proteoglycan content. They consisted of fibers only, with no noticeable beading or fragments. The single-layered PCL scaffolds consisted of a single homogeneous layer, with small pores that were similar in size to the fibers, while the multilayered PCL scaffolds had large, irregular, and unevenly distributed pores.

Staining of acellular CDM scaffolds showed that the fibers contained proteoglycans and small amounts of type II collagen, and that fragments of cartilage of various sizes were present throughout the scaffold. Both singe-layered and multilayered scaffolds contained large, irregular pores, and were not easily distinguishable at the microscale, despite the differences apparent at the macroscale. After 28 days in acellular culture, a slight loss of proteoglycan staining was visible in some cartilage fragments.

ASCs seeded onto all four scaffold types remained on the surface of the scaffolds at day 0. Over 28 days in culture, some of the cells migrated to the interior of the scaffold. In the single-layered PCL scaffolds, cells infiltrated the entire scaffold, but were present at a low density inside of the scaffold with minimal collagen deposition, while a thin layer rich in cells and collagen type II coated the surface of the scaffold. Multilayered PCL scaffolds had superior cellular infiltration, with higher cell density and collagen deposition on the interior of the scaffold than the single-layered scaffolds. There were some areas of tissue overgrowth, but this surface layer smoothly transitioned into the scaffold, in contrast to the sharp interface between the single-layered PCL scaffold and its overgrowth.

After 28 days in culture, single-layered CDM scaffolds had some cellular infiltration near the edges and into large pores, but the inside of the scaffold appeared to remain largely uninhabited. Multilayered CDM scaffolds showed variability in cellular

infiltration, with some showing substantial numbers of cells and significant protein deposition inside of the scaffold, and others where the deposited tissue was only within fissures and pores near the surface. On these CDM scaffolds, the overgrowth contained collagen II but less than the overgrowth on the PCL scaffolds.

It must be noted that many of the scaffolds – particularly multilayered scaffolds – contracted due to the cellular overgrowth. Often this resulted in buckling of the scaffold, resulting in a folded scaffold with a large amount of cellular overgrowth and extracellular matrix deposition inside of the concavity.

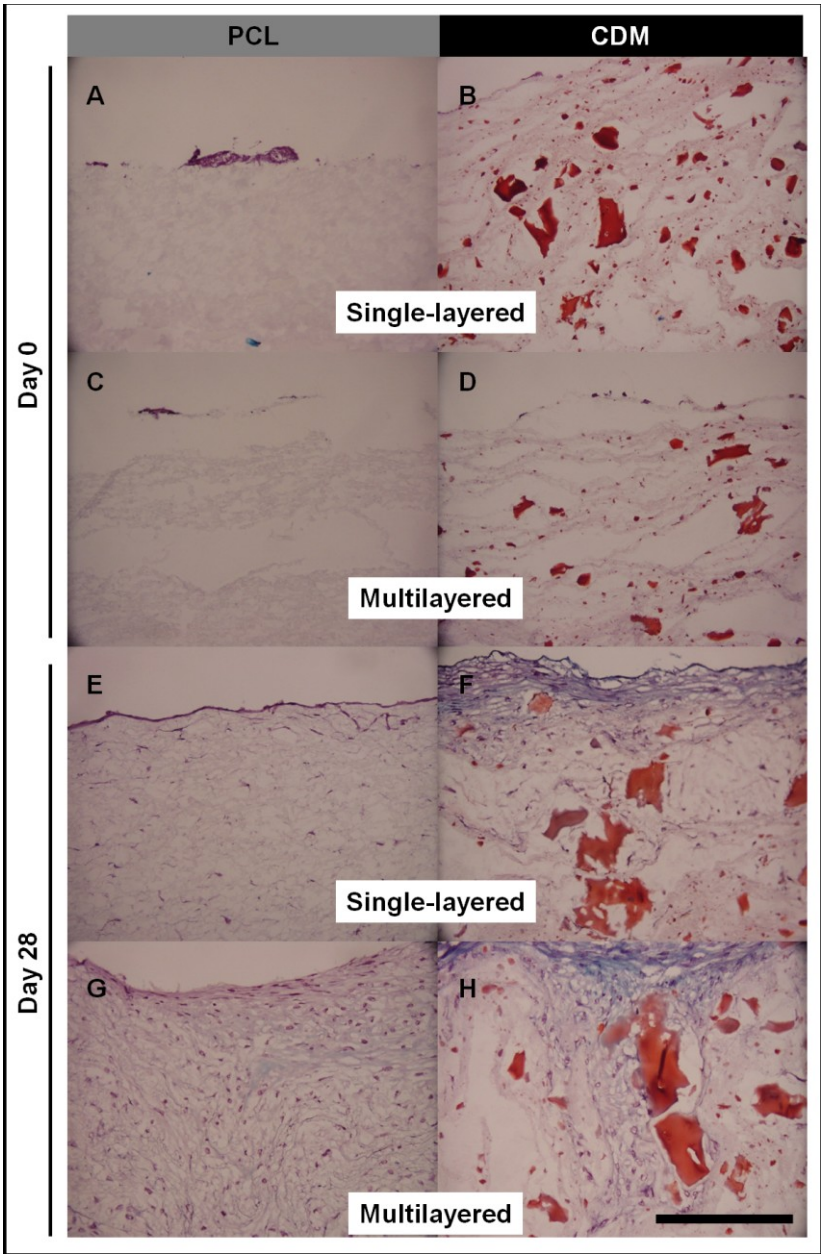


**Figure 14: Scaffolds at day 0 and day 28. (A,B,C,D) Day 0. Nuclei are visible on the surface of the scaffold. PCL scaffolds do not show additional staining. CDM scaffolds show fragments of cartilage and fibers that show proteoglycan staining in single-layered (B) and multilayered (D). After 28 days in culture (E,F,G,H), cells have infiltrated the single-layered PCL (E), but there are more cells and more protein deposition in multilayered PCL (G). Single-layered CDM (F) has primarily cells and tissue on the surface, while multilayered CDM (H) has areas of ingrowth. Scale bar: 250μm**

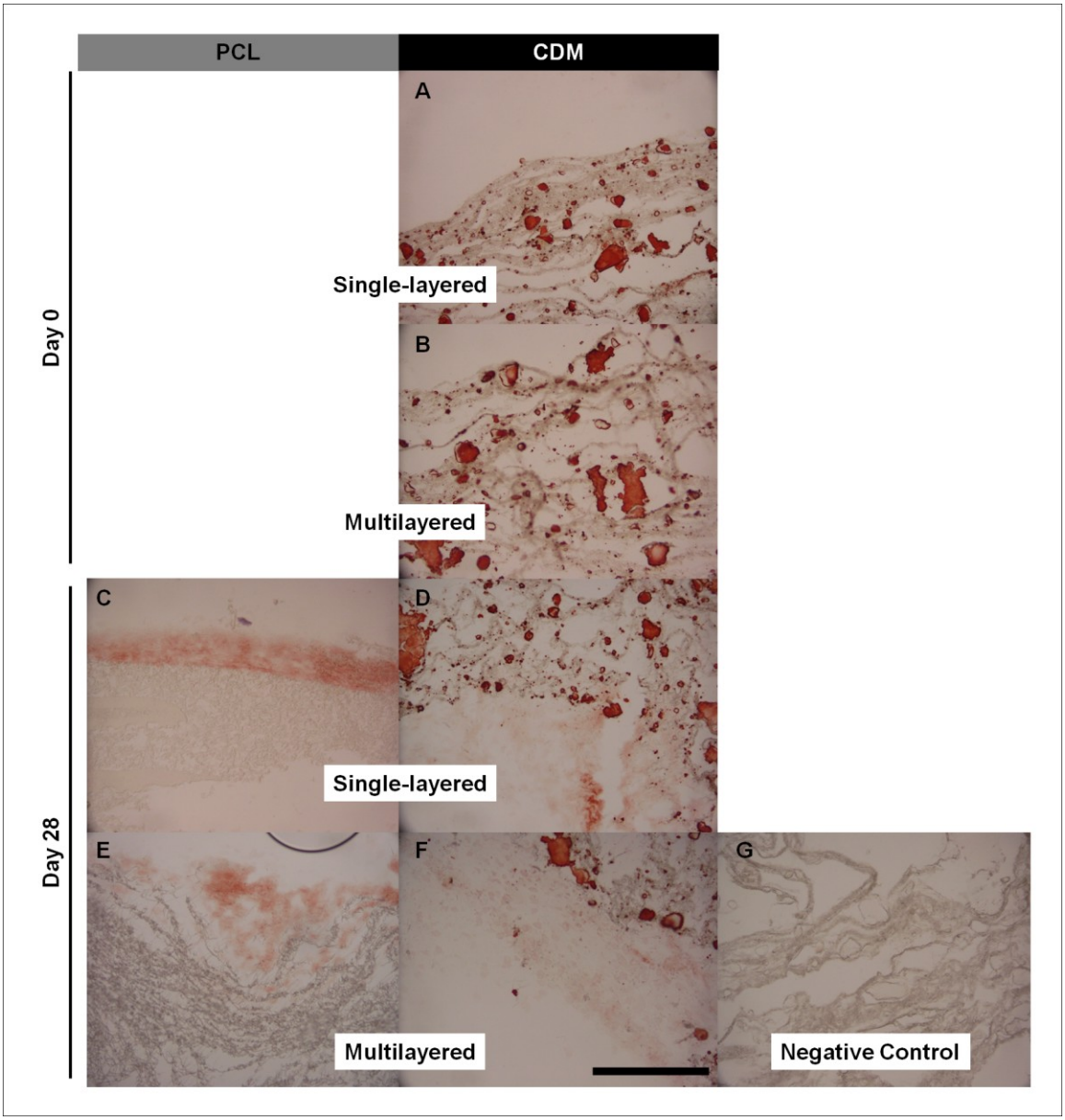


**Figure 15: Collagen II immunohistochemistry. (A,B) Day 0 CDM . Staining visible in cartilage fragments and in fibers. (C,D,E,F) Day 28. PCL scaffolds (C,E) had overgrowth which was more rich in collagen II than CDM scaffolds (D,F). Negative control (G) showed no staining. Day 0 PCL scaffolds were lost in processing. Scale bar: 250μm**

### 3.3.4 Notes on cell seeding

The different materials and structures of the scaffolds resulted in quite different behavior during seeding. Due to the hydrophobic nature of PCL, cells and media remained balanced entirely on the scaffold in the case of the PCL scaffolds, especially the single-layered. The presence of hydrophilic proteins in the CDM scaffolds resulted in the media carrying cells to rapidly be absorbed, contact the tissue culture well, and dissipate some. The void space between the layers of the multilayered PCL scaffolds decreased the effective hydrophobicity and displayed somewhat similar behavior to the CDM scaffolds.

### 3.3.5 Biochemical composition

The scaffolds were quite different in biochemical composition. At day 0, CDM scaffolds contained 2.59 ± 0.10% sulfated glycosaminoglycans by dry weight, as well as 13.24 ± 0.50% collagens by dry weight. PCL scaffolds contained 0.03 ± 0.01% glycosaminoglycans and 0.32 ± 0.20% collagen by dry weight ($p < 0.0001$ for each) at day 0. Over their time in culture, acellular CDM scaffolds decreased from 2.79 ± 0.14% GAG at day 0 to 1.79 ± 0.08% at day 14 to 1.06 ± 0.10% at day 28 ($p < 0.0001$ for all comparisons), while acellular PCL scaffolds continued to have no appreciable glycosaminoglycan content (0.000 ± 0.00% at day 0, 14, and 28; $p > 0.99$) (Figure 16). The same pattern held for collagen content, which decreased in the acellular CDM scaffolds

from 13.78± 0.48% collagen by dry weight at day 0 to 12. 29 ± 0.25% at day 14 to 9.25 ± 0.47% at day 28 ($p < 0.005$), while the acellular PCL scaffolds maintained their negligible level (0.47 ± 0.39% at day 0, 0.07 ± 0.03% at day 14, and 0.07 ± 0.04% at day 28, $p > 0.39$) (Figure 16).

ASCs cultured on the electrospun scaffolds deposited GAGs, increasing the GAG content of cell-seeded PCL constructs to 1.04 ± 0.07% for single-layered PCL and 0.86 ± 0.10% for multilayered PCL at day 28 ($p < 0.0001$), while maintaining a stable GAG content in the multilayered CDM constructs 2.50 ± 0.13% at day 0, increasing to 2.89 ± 0.17% at day 14 and returning to 2.63 ± 0.10% at day 28 (days 0 and 14 different at $p < 0.05$, days 14 and 28 not different $p = 0.10$, days 0 and 28 not different $p = 0.40$). The GAG content of single-layered CDM constructs cultured with ASCs remained stable between day 0 (2.27 ± 0.21%) and day 14 (2.38 ± 0.07%, $p = 0.48$), before decreasing to 1.81 ± 0.15% at day 28 ($p < 0.001$ compared to day 14). At all time points, CDM constructs contained more GAG than PCL constructs.

The multilayered CDM constructs had a higher GAG content than the single-layered constructs when cultured with ASCs at days 14 and 28 ($p < 0.005$ and $p < 0.0001$, respectively). There was no significant difference between single-layered and multilayered structures in the GAG content of PCL constructs at any time point ($p > 0.24$).

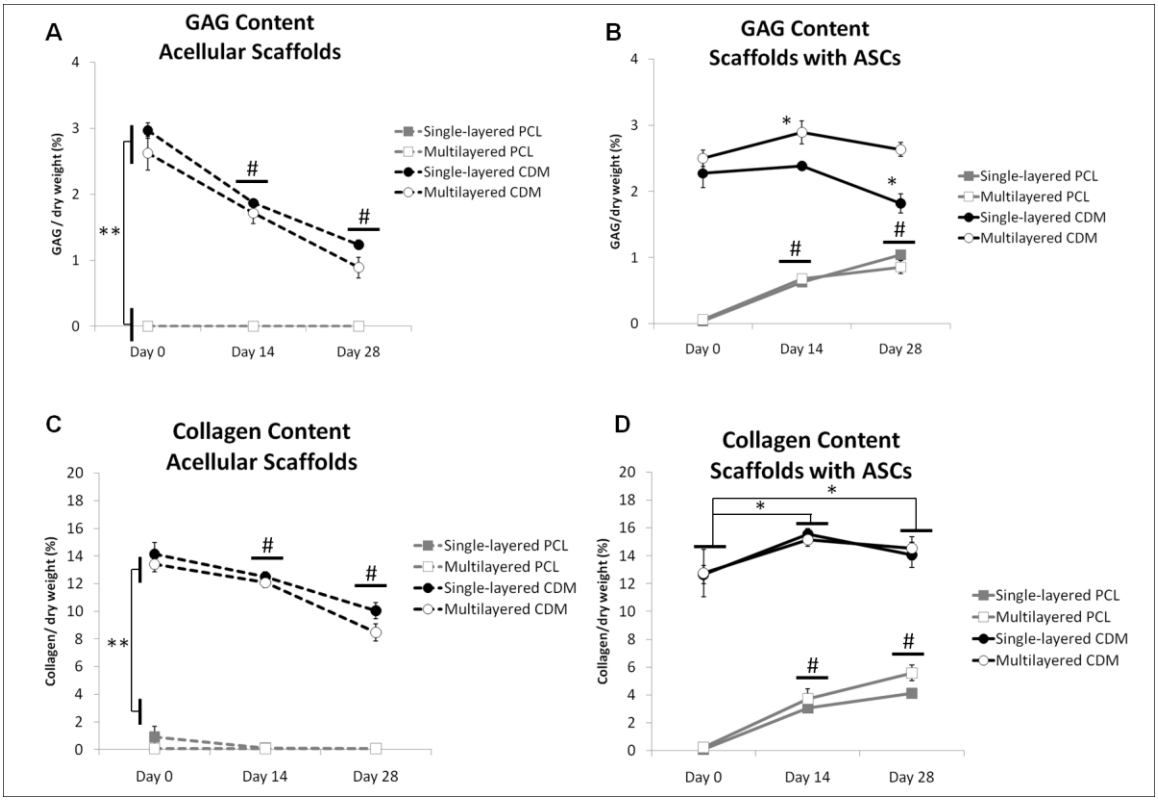


**Figure 16: Extracellular matrix components (A) sulfated glycosaminoglycans and (C) collagen are present in CDM scaffolds, but decrease with time acellular scaffolds. When cultured with ASCs, (B) sulfated glycosaminoglycans increase temporarily in multilayered scaffolds while decreasing slightly in single-layered scaffolds. Collagen content increases in both CDM and PCL scaffolds. CDM scaffolds have higher protein content than PCL for all groups and time points. *Different from day 0 $p<0.05$; **$p<0.0001$ ;#Different from previous time point $p<0.05$. Bars denote grouping points together.**

Collagens were also deposited by ASCs in all scaffold types. The PCL constructs increased from 0.16 ± 0.07% at day 0 to 3.40 ± 0.38% at day 28 ($p < 0.0001$). CDM constructs increased from 12.70 ± 0.86% at day 0 to 15.35 ± 0.30% at day 14 ($p < 0.0005$), and did not change significantly over the final 14 days, being 14.29 ± 0.60% at day 28 ($p =$

0.15 compared to day 14, $p < 0.05$ compared to day 0). The presence or absence of multiple layers did not affect collagen deposition (main effect of layers: $p = 0.33$).

Double-stranded DNA content, a proxy for cell number, increased for all scaffold types, and was significantly higher in cell-seeded scaffolds at day 0 (1583 ± 208 ng) than in the acellular scaffolds (130 ± 18 ng)[2] ($p < 0.0001$). Immediately after seeding, the PCL scaffolds had 2109 ± 309 ng DNA, significantly more than the 1056 ± 186 ng on the CDM scaffolds ($p < 0.0001$). Additionally, single-layered scaffolds had more DNA at day 0 (2036 ± 315 ng) than the multilayered scaffolds did (1130 ± 209 ng) ($p < 0.005$). These differences persisted throughout the 28 days in culture ($p < 0.0001$).

[2] The DNA content of the acellular groups (which average 96 ± 7 ng DNA) is significantly overestimated, due to the effects of fitting a line to standard dilutions over multiple orders of magnitude,

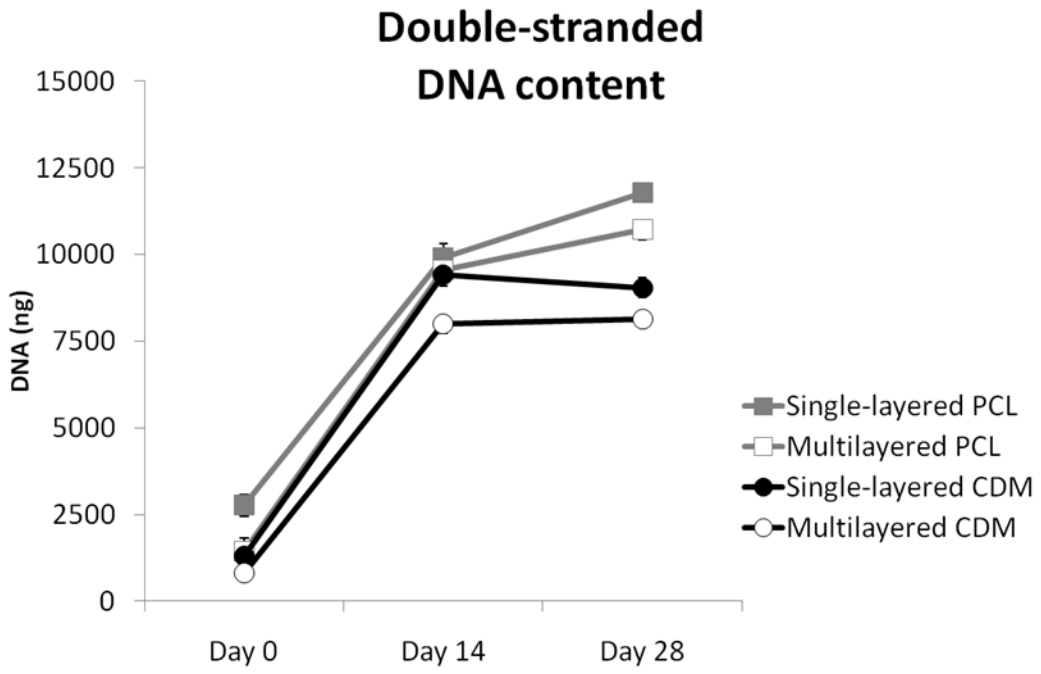


**Figure 17: Double stranded DNA content, used as a proxy for cell number. DNA on CDM scaffolds did not increase between day 14 and day 28 (p=0.71), but did for all scaffold types in the first 14 days and for PCL scaffolds between days 14 and 28. PCL scaffolds had more cells bound at day 0 compared to CDM, as did single-layered scaffolds compared to multilayered ($p < 0.005$). This difference persisted at all time points.**

DNA increased in all cell-seeded groups during the first 14 days to 9219 ± 210 ng DNA ($p < 0.0001$). Over the next 14 days, ASCs on PCL scaffolds proliferated (9910 ± 392 ng DNA on day 14 to 11884 ± 229 ng on day 28 for single-layered scaffolds, $p < 0.0001$; 9550 ± 251 ng to 10717 ± 283 ng DNA for multilayered scaffolds, $p < 0.01$), while cells on CDM scaffolds did not proliferate (9426 ± 324 ng DNA on day 14 to 9044 ± 290 on day 28 for single-layered CDM, $p = 0.36$; 7992 ± 251 ng to 8144 ± 190 ng DNA for multilayered scaffolds, $p = 0.71$).

### 3.3.6 Gene expression

CDM scaffolds induced increases expression of chondrogenic genes. COL2 gene expression at day 0, showing a 29-fold increase over the day 0 cells (which were not exposed to any scaffold), compared to a 6-fold increase in the PCL scaffolds ($p < 0.0001$). This difference disappeared by day 1, after which the scaffolds showed similar COL2 expression profiles. By day 14, CDM scaffolds also induced greater ACAN expression (327 times the day 0 cellular control) than the PCL scaffolds did (257 times control) ($p < 0.01$). In addition to these genes indicating healthy cartilage phenotype, COL10 expression was also higher in CDM scaffolds at day 14 (36 times control) than it was in PCL scaffolds (26 times control) ($p < 0.0001$).

Multilayered structures also increased the expression of some genes. ACAN expression was higher in multilayered scaffolds at day 14 (337 times the day 0 cellular control) than single-layered scaffolds (247 times control) ($p = 0.007$). Across all time points, multilayered scaffolds expressed more COL1 (4.0 times control) than single-layered scaffolds (2.8 times control) ($p < 0.05$), and multilayered CDM caused higher COL1 expression than other scaffold types ($p < 0.05$).

Aside from COL2, expression levels of other genes analyzed increased with time in culture during the first 14 days. ACAN expression was up 134-fold at day 7 (different from all previous time points, $p < 0.0001$), and 292-fold at day 14 (different from all previous time points, $p < 0.0001$). COL1peaked at day 7 at a 7-fold increase (different

from all other time points, $p < 0.05$), before returning at day 14 to a 5-fold increase over the day 0 cellular control (different from all other time points, $p < 0.05$). COL10 showed a rapid increase, with days 3, 7, and 14 all being higher than all previous time points ($p < 0.005$), reaching a 31-fold upregulation by day 14.

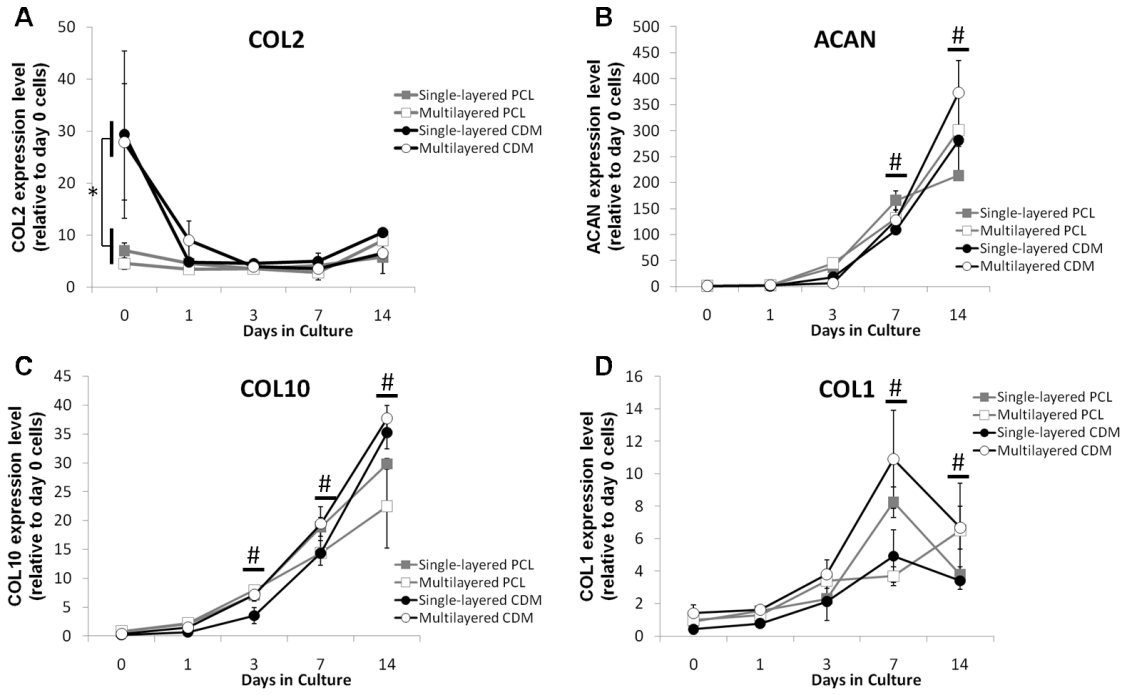


**Figure 18: Gene expression relative to day 0 cellular control. (A) COL2 expression is higher in CDM scaffolds than PCL at day 0. (B) ACAN expression rises at days 7 and 14. At day 14, ACAN expression is higher in CDM than PCL, and higher in multilayered than single-layered. (C) COL10 expression rises at days 3, 7, 14, and is higher n multilayered scaffolds than single-layered. (D) COL1 expression peaks at day 7 and is higher in multilayered scaffolds than single-layered. Multilayered CDM scaffolds had more COL1 expression than other scaffolds. #Different from all other time points ($p<0.05$). Bars denote grouping points together.**

## *3.4 Discussion*

Our findings present a novel method for incorporating unpurified proteins from a solid tissue into the fibers of electrospun scaffolds for tissue engineering, as well as an improved method for enhancing cellular infiltration into a tissue engineering scaffold. This material prompted some chondrogenic gene expression immediately upon seeding. Additionally, multilayered scaffolds showed improved cellular infiltration and extracellular matrix deposition.

### 3.4.1 Electrospun Cartilage-Derived Matrix

The method of electrospinning cartilage-derived matrix described here functions as a proof-of-principle that native proteins can be harvested from a solid tissue and electrospun into fibrous scaffolds for tissue engineering without purification, as the cartilage-derived proteins are incorporated into the fibers of the scaffold itself. Previously, electrospinning of purified proteins, particularly collagen, was an attractive technique for fabricating tissue engineering scaffolds,(Matthews, Wnek et al. 2002; Boland, Matthews et al. 2004; Shields, Beckman et al. 2004; Zhong, Teo et al. 2005; Zhong, Teo et al. 2007) as an adaptation of the earlier technique of using tissue-derived matrices such as demineralized bone, (Urist 1965) small intestinal submucosa, (Badylak, Lantz et al. 1989) or, more recently, cartilage-derived matrix(Cheng, Estes et al. 2009; Cheng, Estes et al. 2011). However, previous works electrospinning tissue-derived proteins have required protein purification, which may remove important components

or alter protein conformations. Only very recently have unpurified proteins been electrospun with platelet-rich plasma (Sell, Wolfe et al. 2011), but no one has previously electrospun solid tissue.

Cartilage proteins were present in the fibers of electrospun cartilage-derived matrix scaffolds, in addition to being present as fragments of undissolved cartilage, as cartilage proteins made up 15% of the scaffold by dry weight. Their concentration of collagen was 5 times as high as proteoglycan, a similar ratio to articular cartilage, which consists of 2-4 times as much collagen as proteoglycan.(Mow and Huiskes 2005) The similarity of this ratio indicates that neither of the two major cartilage component is being substantially lost in the lyophilizing, pulverizing, filtering, and electrospinning process.

Over time, the cartilage extracellular matrix proteins present in the CDM scaffolds diminished, likely leaching out into the culture media, as evidenced by the decreasing protein content in the acellular CDM scaffolds. However, it must be noted that the ASCs deposited extracellular matrix proteins at a similar rate to the leaching, allowing the scaffold to maintain a similar composition of 2-3% proteoglycans and 12-15% collagen. This is important to the development of tissue-engineering scaffolds, as one paradigm of tissue engineering is to engineer a scaffold with similar properties to the target tissue, and allow the cells to fill in and remodel the scaffold.

The electrospun cartilage-derived matrix scaffolds exhibited somewhat of a chondrogenic effect on adipose stem cells when compared to the scaffolds made from purely synthetic polymer. Within a few hours on the CDM scaffold, collagen II expression was significantly upregulated, though it did not persist, indicating that the CDM presence in the scaffolds had a chondrogenic effect on the cells, but that this effect was short-lived compared to the sustained collagen II increase seen in previous CDM scaffolds.(Cheng, Estes et al. 2009) Because previous studies have employed transwells to show that the chondrogenic nature of CDM comes from direct cell-matrix interaction rather than soluble factors which would quickly diminish, the decreasing chondrogenic effect is likely due to growth factors in the media overwhelming the effects of the scaffold.

All scaffolds showed an increase in aggrecan expression scaffolds over 14 days in culture, along with an increase in expression of fibrocartilage markers collagens I and X, though the effect was stronger in the CDM scaffolds. Previous work with non-electrospun CDM showed no increase in collagens I or X.(Cheng, Estes et al. 2009) The increases in collagens I and X are largely due to the fibrous nature of electrospun scaffolds. ASCs attach to the fibers and expand along them, giving a flattened or elongated shape, rather than the rounded shape that is necessary for articular cartilage production.(Li, Mauck et al. 2007; Garrigues, Little et al. 2010; Estes and Guilak 2011) The interior of the scaffolds did not show any deposited collagen II, in contrast to the

areas of overgrown tissue, indicating that the fibrous morphology of the scaffolds and therefore elongation of the cells may be causing the cells to produce collagen I rather than collagen II, while the overgrowth areas allow for a more rounded cell shape and collagen II production. The increased aggrecan gene expression seen in our scaffolds was due to the presence of chondrogenic growth factors, as BMP-6 has been shown to increase aggrecan expression.(Estes, Wu et al. 2006)

Additionally, some phenotypic differences between ASCs on CDM and PCL scaffolds persist. For example, ASCs on the CDM scaffold did not proliferate between 14 and 28 days, while cells on the PCL scaffolds did, albeit at a slower rate than the first 14 days. This study did not determine whether this halt in proliferation indicates an increase in extracellular matrix production, but it is likely a result of either differences in cell-scaffold attachment and interaction or a difference in the architecture of cell buildup, as the CDM scaffolds had more dense cell- and ECM-rich regions.

### 3.4.2 Multilayered scaffolds

Multilayered scaffolds allowed improved cellular infiltration and increased interior extracellular matrix deposition, when compared to single-layered scaffolds. This was especially true for multilayered PCL scaffolds. Previous multilayered scaffolds have been vacuum expanded to ten times their previous thickness, greatly increasing the porosity of the scaffold and decreasing the tortuosity of the pores, thus allowing increased cell penetration.(Tzezana, Zussman et al. 2008) We have shown that vacuum

expansion is not required to greatly increase the cellular penetration of multilayered scaffolds, resulting in much more homogeneous extracellular matrix deposition throughout the thickness of the scaffold. Additionally, using multilayered scaffolds without vacuum expansion does not sacrifice the advantages that this technique has over other methods to increase cellular penetration, such as vacuum infusion and forming the scaffold from loose electrospun fibers centrifuged with cells.(Li, Jiang et al. 2008; Chen, Michaud et al. 2009) Consistent extracellular matrix deposition throughout the thickness of the scaffold is crucial for an engineered biomechanical tissue which will eventually be required to hold compressive loads.

The described method of producing multilayered scaffolds introduces the ability to control the properties of each layer – different materials or fiber alignments in neighboring layers would allow new types of composites to be used while improving cellular infiltration and ECM deposition on the interior of the scaffold. Now that we have shown that these scaffolds do not need to be vacuum expanded, tissue engineers can take advantage of the improved cellular penetration and controllability of these scaffolds without requiring such thick scaffolds with large void spaces and extremely low density.

Multilayered scaffolds also caused increased aggrecan gene expression, and, in the case of multilayered CDM scaffolds, more proteoglycan accumulation. On the other

hand, multilayered scaffolds showed higher collagen I expression despite the chondrogenic media culture conditions.

Cartilage fragments were present in the scaffold, along with the composite CDM fibers. These fragments were rich in cartilage proteins, but also had a substantial effect on scaffold structure. The fragments which prohibited good integration of the fibers laid down immediately following the fragment deposition by acting as a support, effectively creating an areas within the single-layered scaffolds that was quite similar to the separation between layers in the multilayered scaffold. These pores within the single-layered scaffold were opened upon histological sectioning, causing the single-layered CDM scaffolds to look quite similar to multilayered scaffolds when analyzed in cross-section, despite being visibly different from the macroscale. Also, the fragments were coated in solvent as they were deposited, allowing them to penetrate previously deposited fibers and create additional large pores as they pass through the other layers. This explains the presence of fragments despite the fact that they were not visible from the surface via SEM – these fragments were covered by a layer of fibers.

It must be noted that others have reported superior cellular attachment in scaffolds containing collagen, in contrast to our data showing more ASCs initially attaching to the PCL scaffold.(Zhang, Venugopal et al. 2005) Though the mechanics of cellular attachment to the matrix may also be involved, this was largely the result of the fluid mechanics of the seeding media. The hydrophobic PCL scaffolds held the cell

suspension, allowing all of the cells to settle onto the scaffold, whereas the partially hydrophilic CDM scaffolds could not hold the drop of cell suspension, causing the cells to escape the scaffold before they were able to attach. This difference in cellular attachment at seeding persisted throughout the constructs' time in culture.

### 3.4.3 Conclusion

The incorporation of unpurified proteins from a solid tissue into the fibers of electrospun scaffolds is an important step in the development of engineered tissue. We have accomplished this with electrospun cartilage-derived matrix and shown that these scaffolds have chondrogenic potential. We have also demonstrated an improved method for enhancing cellular infiltration into a tissue engineering scaffold.

# 4. Conclusions

## *4.1 Summary*

The aim of this dissertation was to develop new techniques for producing electrospun scaffolds for use in the tissue engineering of articular cartilage. Electrospinning was chosen as a primary technology due to the small diameter of the fibers, which have been shown to have advantageous properties both *in vitro* and *in vivo*. From there, we developed techniques that allowed the control of mechanical properties and the improvement of cellular infiltration, as well as a novel chondrogenic material and a better understanding of the nature of fiber alignment and its effect on cell alignment within electrospun scaffolds.

First, we developed a novel method of imparting mechanical anisotropy to electrospun scaffolds that allowed the production of a single, cohesive scaffold with varying directions of anisotropy in different layers by employing insulating masks to control the electric field. Previous methods of electrospinning anisotropic scaffolds only allowed a single direction of fiber alignment, meaning that in order to produce a scaffold with varying directions of anisotropy, multiple scaffolds had to be made and attached together. The production of scaffolds with multiple directions of anisotropy is an important step towards the functional tissue engineering of many tissues. Intervertebral discs possess layers with collagen fiber alignment at ±30°, and articular cartilage shows significant anisotropy in the surface layer transitioning to transverse isotropy in the

deep zone. Additionally, the use of insulating masks allows the production of scaffolds with a lower level of anisotropy than is achievable with most other methods, which are quite similar to the anisotropy levels in articular cartilage.

Next, we improved the quantification of fiber alignment, making it much more sensitive than previous methods. In this process, we discovered that the surface fibers in the isotropic scaffolds showed similar amounts of fiber alignment as some types of anisotropic scaffolds. The difference was in the direction of alignment, where the anisotropic scaffolds consistently showed preferential alignment in the expected direction (the direction of greatest stiffness in tension), and the isotropic scaffolds showed subtle alignment, but in an unpredictable direction.

The presence of subtle alignment in the surface of all of our electrospun scaffolds, whether isotropic or anisotropic, was confirmed by the behavior of adipose stem cells cultured on the scaffolds. We found that cells preferentially aligned themselves along the stiffer axis of the anisotropic scaffolds, despite the necessity of the analysis above to perceive the fiber alignment. Additionally, we found that cells preferentially aligned themselves to a similar degree on the surface of the isotropic scaffolds, but the direction of this alignment again varied from scaffold to scaffold.

The fiber alignment of isotropic scaffolds, which we were the first to describe, could be explained by fibers which stretch out in opposite directions during the whipping phase, resulting in fibers which have a slight preference towards parallel

alignment. This parallel alignment likely changes orientation with time in the isotropic scaffolds but remains steady in the anisotropic scaffolds. Imaging of the interior of the electrospun scaffolds, currently not feasible due to their density and the associated scattering and attenuation of the signal, when combined with the fiber alignment analysis methods developed here, would allow the calculation of the fiber alignment throughout the thickness of a single scaffold. This would allow the testing of our hypothesis of local alignment which varies over time (and therefore, depth) in the isotropic scaffolds, while remaining constant in the anisotropic scaffolds. Further, longer-term culture of ASCs on the scaffolds to achieve some infiltration would allow the analysis of how cells align themselves in response to the varying alignments, particularly when a single cell is exposed to multiple directions of aligned fibers on different sides.

Next, we approached the problem of insufficient cellular infiltration that has plagued electrospun scaffolds. Multilayered scaffolds, collected on a water bath and not expanded with a vacuum, showed marked improvement in allowing cells to migrate to the interior of the scaffold. A much higher density of cells was present on the interior of the multilayered scaffolds than the single-layered scaffolds which are typically used for tissue engineering in the literature. Moreover, this increased cell density inside of the scaffold resulted in more extracellular matrix deposition inside of the scaffold. It must be noted that this layering should be supplemented with additional technologies that

avoid folding or buckling due to cell-mediated contraction. Additionally, the pores within the multilayered scaffold were not completely filled with extracellular matrix, resulting in a less stiff construct compared to the single-layered scaffold. Further time in culture may fill these pores and increase the mechanical stiffness up to the level of the single-layered scaffold.

Finally, we electrospun a new material that incorporates native cartilage proteins. This cartilage-derived matrix and poly(ε-caprolactone) composite scaffold had had collagen II and proteoglycan incorporated into the fibers. At production, it was 15% collagen and proteoglycan by dry weight, and was able to maintain this level as the cells deposited extracellular matrix at a similar rate to the leaching of protein into the media. Because these scaffolds already contain significant proteoglycan content when initially seeded with cells, this may allow the more rapid development of viscoelastic mechanical properties similar to cartilage. This cartilage-derived material appears to have chondrogenic potential, as it caused upregulation of collagen II gene expression in ASCs within the first few hours of contact with the scaffold. However, media and cell type optimization would enhance the utility of this material, as the initial collagen II response disappeared, and was likely overwhelmed by the interaction between the cells and growth factors over time.

## 4.2 Future directions

In the course of performing the experiments that led to this dissertation, many other discoveries were made, ideas were hatched, and experiments were designed. While some have been mentioned above as the logical next step to test a hypothesis that grew out of the experiments described in this work, many others were tangential and merely inspired by them. These ideas have already been executed to varying degrees, and some remain merely ideas.

The combination of an electrospun scaffold with a more porous woven scaffold would improve both scaffolds. The woven scaffold would provide stiffer mechanical properties and immediate delivery of cells to the scaffold center upon seeding. The electrospun scaffold could aid in lowering the coefficient of friction and decreasing wear of the opposing cartilage face at early time points before cellular overgrowth lubricates the entire construct. This lowering of friction and wear could allow for the implantation of the construct into a patient with less time in culture. We developed a method of binding these two scaffold types with minimal destruction of either type, but much more analysis needs to be performed.

The addition of other materials to an electrospun scaffold is fertile ground for future improvements in tissue engineering. While previous studies, including ours, have focused on adding the materials to the electrospinning material (by mixing it in the solution to be spun, adding it in a core-sheath configuration, spinning it from a second

needle, etc.), it could also be added at the collecting site, particularly when the collecting site is a fluid bath. This could lead to fibers which are cross-linked or chemically functionalized as soon as they are deposited. Another possibility is to collect the fibers in a bath of a concentrated hygroscopic material to allow the soaking of the finished scaffold in cell culture media, resulting in expansion of the gel, which would provide unique mechanical properties, as it would create an electrospun scaffold infused with gel, where the fibers were under a preload. This initial expansion could be used to aid in the cell infusion at seeding. Drugs or other functional molecules which are present in high concentrations in the collecting solution will be bound to the surface of the fibers, as the fibers are not fully solidified when they reach the collecting bath. We have shown proof-of-concept in the addition of proteins via the collecting bath.

## *4.3 Conclusion*

Taken together, this dissertation has presented a broad look at techniques to improve the electrospinning process, specifically with the intent of enhancing the use of electrospun scaffolds for the tissue engineering of artificial cartilage. This was done through an analysis of the structure of electrospun scaffolds, how these structures affect cells, and how to influence these structures to control the mechanical properties in new ways, as well as developing a method for electrospinning fibers made from native, unpurified cartilage tissue. We studied the processing of materials before they are electrospun (in developing a solution that would be suitable), during the electrospinning

process (ensuring that CDM formed good fibers and that we could align the fibers to create mechanical anisotropy), and after electrospinning (culturing cells on electrospun scaffolds), and made advancements in all three phases.

# References


Ateshian, G. A. and C. T. Hung (2003). Functional Properties of Native Articular Cartilage. Functional Tissue Engineering. F. Guilak, D. L. Butler, S. A. Goldstein and D. J. Mooney. New York, Springer -Verlag**:** 46-68.

Ayres, C., G. L. Bowlin, et al. (2006). "Modulation of anisotropy in electrospun tissue-engineering scaffolds: Analysis of fiber alignment by the fast Fourier transform." Biomaterials **27**(32): 5524-5534.

Ayres, C. E., G. L. Bowlin, et al. (2007). "Incremental changes in anisotropy induce incremental changes in the material properties of electrospun scaffolds." Acta Biomaterialia **3**(5): 651-661.

Ayres, C. E., B. S. Jha, et al. (2008). "Measuring fiber alignment in electrospun scaffolds: a user's guide to the 2D fast Fourier transform approach." J Biomater Sci Polym Ed **19**(5): 603-21.

Badylak, S. F., G. C. Lantz, et al. (1989). "Small intestinal submucosa as a large diameter vascular graft in the dog." J Surg Res **47**(1): 74-80.

Baker, B. M. and R. L. Mauck (2007). "The effect of nanofiber alignment on the maturation of engineered meniscus constructs." Biomaterials **28**(11): 1967-77.

Baker, B. M., A. S. Nathan, et al. (2009). "Tissue engineering with meniscus cells derived from surgical debris." Osteoarthritis and Cartilage **17**(3): 336-345.

Below, S., S. P. Arnoczky, et al. (2002). "The split-line pattern of the distal femur: A consideration in the orientation of autologous cartilage grafts." Arthroscopy **18**(6): 613-7.

Boland, E. D., J. A. Matthews, et al. (2004). "Electrospinning collagen and elastin: preliminary vascular tissue engineering." Front Biosci **9**: 1422-32.

Buckwalter, J. A. and J. A. Martin (2006). "Osteoarthritis." Advanced Drug Delivery Reviews **58**(2): 150-167.

Buckwalter, J. A., C. Saltzman, et al. (2004). "The impact of osteoarthritis - Implications for research." Clinical Orthopaedics and Related Research(427): S6-S15.

Butler, D. L., S. A. Goldstein, et al. (2000). "Functional tissue engineering: the role of biomechanics." J Biomech Eng **122**(6): 570-5.

Buttafoco, L., N. G. Kolkman, et al. (2006). "Electrospinning of collagen and elastin for tissue engineering applications." Biomaterials **27**(5): 724-34.

Cao, H., K. Mchugh, et al. (2010). "The topographical effect of electrospun nanofibrous scaffolds on the *in vivo* and *in vitro* foreign body reaction." Journal of Biomedical Materials Research Part A **93A**(3): 1151-1159.

Carnell, L. S., E. J. Siochi, et al. (2008). "Aligned Mats from Electrospun Single Fibers." Macromolecules **41**(14): 5345-5349.

Casper, C. L., N. Yamaguchi, et al. (2005). "Functionalizing Electrospun Fibers with Biologically Relevant Macromolecules." Biomacromolecules **6**(4): 1998-2007.

CDC. (2011). "Arthritis." Retrieved March 2010, from http://www.cdc.gov/arthritis/.

Chakraborty, S., I. C. Liao, et al. (2009). "Electrohydrodynamics: A facile technique to fabricate drug delivery systems." Advanced Drug Delivery Reviews **61**(12): 1043-1054.

Chen, M., H. Michaud, et al. (2009). "Controlled Vacuum Seeding as a Means of Generating Uniform Cellular Distribution in Electrospun Polycaprolactone (PCL) Scaffolds." Journal of Biomechanical Engineering **131**(7): 074521.

Cheng, N.-C., B. T. Estes, et al. (2011). "Engineered cartilage using primary chondrocytes cultured in a porous cartilage-derived matrix." Regenerative Medicine **6**(1): 81-93.

Cheng, N. C., B. T. Estes, et al. (2009). "Chondrogenic differentiation of adipose-derived adult stem cells by a porous scaffold derived from native articular cartilage extracellular matrix." Tissue Eng Part A **15**(2): 231-41.

Chew, S. Y., R. Mi, et al. (2007). "Aligned Protein–Polymer Composite Fibers Enhance Nerve Regeneration: A Potential Tissue-Engineering Platform." Advanced Functional Materials **17**(8): 1288-1296.

Chew, S. Y., R. Mi, et al. (2008). "The effect of the alignment of electrospun fibrous scaffolds on Schwann cell maturation." Biomaterials **29**(6): 653-661.

Chew, S. Y., J. Wen, et al. (2005). "Sustained Release of Proteins from Electrospun Biodegradable Fibers." Biomacromolecules **6**(4): 2017-2024.

Choi, J. S., S. J. Lee, et al. (2008). "The influence of electrospun aligned poly(epsilon-caprolactone)/collagen nanofiber meshes on the formation of self-aligned skeletal muscle myotubes." Biomaterials **29**(19): 2899-906.

Christenson, E. M., K. S. Anseth, et al. (2007). "Nanobiomaterial applications in orthopedics." Journal of Orthopaedic Research **25**(1): 11-22.

Coleman, S. H., R. Malizia, et al. (2001). "Treatment of isolated articular cartilage lesions of the medial femoral condyle. A clinical nad MR comparison of autologous chondrocyte implantation vs. microfracture." Ortop Traumatol Rehabil **3**(2): 224-6.

Courtney, T., M. S. Sacks, et al. (2006). "Design and analysis of tissue engineering scaffolds that mimic soft tissue mechanical anisotropy." Biomaterials **27**(19): 3631-8.

Deitzel, J. M., J. Kleinmeyer, et al. (2001). "The effect of processing variables on the morphology of electrospun nanofibers and textiles." Polymer **42**(1): 261-272.

Dong, B., O. Arnoult, et al. (2009). "Electrospinning of Collagen Nanofiber Scaffolds from Benign Solvents." Macromolecular Rapid Communications **30**(7): 539-542.

Doshi, J. and D. H. Reneker (1995). "Electrospinning process and applications of electrospun fibers." Journal of Electrostatics **35**(2-3): 151-160.

Eichhorn, S. J. and W. W. Sampson (2005). "Statistical geometry of pores and statistics of porous nanofibrous assemblies." Journal of The Royal Society Interface **2**(4): 309-318.

Estes, B. T. and F. Guilak (2011). "Three-dimensional culture systems to induce chondrogenesis of adipose-derived stem cells." Methods Mol Biol **702**: 201-17.

Estes, B. T., A. W. Wu, et al. (2006). "Potent induction of chondrocytic differentiation of human adipose-derived adult stem cells by bone morphogenetic protein 6." Arthritis & Rheumatism **54**(4): 1222-1232.

Formhals, A. (1934). Process and apparatus for preparing artificial threads, US Patent Office. **1,975,504**.

Garrigues, N. W., D. Little, et al. (2010). "Use of an insulating mask for controlling anisotropy in multilayer electrospun scaffolds for tissue engineering." J Mater Chem **20**(40): 8962-8968.

Guilak, F., D. M. Cohen, et al. (2009). "Control of Stem Cell Fate by Physical Interactions with the Extracellular Matrix." Cell Stem Cell **5**(1): 17-26.

Guilak, F., K. E. Lott, et al. (2006). "Clonal analysis of the differentiation potential of human adipose-derived adult stem cells." Journal of Cellular Physiology **206**(1): 229-237.

Hangody, L., G. Kish, et al. (1997). "Arthroscopic autogenous osteochondral mosaicplasty for the treatment of femoral condylar articular defects A preliminary report." Knee Surgery, Sports Traumatology, Arthroscopy **5**(4): 262-267.

Hong, S. and G. Kim (2010). "Electrospun micro/nanofibrous conduits composed of poly(ε-caprolactone) and small intestine submucosa powder for nerve tissue regeneration." Journal of Biomedical Materials Research Part B: Applied Biomaterials **94B**(2): 421-428.

Hong, S. and G. H. Kim (2010). "Electrospun Polycaprolactone/Silk Fibroin/Small Intestine Submucosa Composites for Biomedical Applications." Macromolecular Materials and Engineering **295**(6): 529-534.

Huang, C.-Y., A. Stankiewicz, et al. (1999). "Anisotropy, inhomogeneity, and tension-compression nonlinearity of human glenohumeral cartilage in finite deformation." Transactions of the Orthopaedic Research Society **24**: 95.

Hwang, C., Y. Park, et al. (2009). "Controlled cellular orientation on PLGA microfibers with defined diameters." Biomedical Microdevices **11**(4): 739-746.

Jaeger, D., J. Schischka, et al. (2009). "Tensile testing of individual ultrathin electrospun poly(L-lactic acid) fibers." Journal of Applied Polymer Science **114**(6): 3774-3779.

Jayasinghe, S. N. and A. Townsend-Nicholson (2006). "Stable electric-field driven cone-jetting of concentrated biosuspensions." Lab Chip **6**(8): 1086-90.

Kempson, G. E., M. A. R. Freeman, et al. (1968). "Tensile Properties of Articular Cartilage." Nature **220**(5172): 1127-1128.

Kempson, G. E., H. Muir, et al. (1973). "The tensile properties of the cartilage of human femoral condyles related to the content of collagen and glycosaminoglycans." Biochimica et Biophysica Acta (BBA) - General Subjects **297**(2): 456-472.

Kim, G. H. (2008). "Electrospun PCL nanofibers with anisotropic mechanical properties as a biomedical scaffold." Biomed Mater **3**(2): 25010.

Kim, J.-S. and D. H. Reneker (1999). "Mechanical Properties of Composites Using Ultrafine Electrospun Fibers." Polymer Composites **20**(1): 124-131.

Kim, T. G., H. J. Chung, et al. (2008). "Macroporous and nanofibrous hyaluronic acid/collagen hybrid scaffold fabricated by concurrent electrospinning and deposition/leaching of salt particles." Acta Biomaterialia **4**(6): 1611-1619.

Knutsen, G., J. O. Drogset, et al. (2007). "A randomized trial comparing autologous chondrocyte implantation with microfracture. Findings at five years." J Bone Joint Surg Am **89**(10): 2105-12.

Kumbar, S. G., R. James, et al. (2008). "Electrospun nanofiber scaffolds: engineering soft tissues." Biomedical Materials **3**(3): 034002.

Kumbar, S. G., S. P. Nukavarapu, et al. (2008). "Electrospun poly(lactic acid-co-glycolic acid) scaffolds for skin tissue engineering." Biomaterials **29**(30): 4100-4107.

Lee, K. H., H. Y. Kim, et al. (2003). "Characterization of nano-structured poly([var epsilon]-caprolactone) nonwoven mats via electrospinning." Polymer **44**(4): 1287-1294.

Li, C., C. Vepari, et al. (2006). "Electrospun silk-BMP-2 scaffolds for bone tissue engineering." Biomaterials **27**(16): 3115-3124.

Li, D., J. T. McCann, et al. (2005). "Use of Electrospinning to Directly Fabricate Hollow Nanofibers with Functionalized Inner and Outer Surfaces13." Small **1**(1): 83-86.

Li, D., G. Ouyang, et al. (2005). "Collecting electrospun nanofibers with patterned electrodes." Nano Lett **5**(5): 913-6.

Li, D., Y. Wang, et al. (2003). "Electrospinning of Polymeric and Ceramic Nanofibers as Uniaxially Aligned Arrays." Nano Letters **3**(8): 1167-1171.

Li, D., Y. Wang, et al. (2004). "Electrospinning Nanofibers as Uniaxially Aligned Arrays and Layer-by-Layer Stacked Films." Advanced Materials **16**(4): 361-366.

Li, D. and Y. Xia (2004). "Electrospinning of Nanofibers: Reinventing the Wheel?" Advanced Materials **16**(14): 1151-1170.

Li, W.-J., Y. J. Jiang, et al. (2008). "Cell--Nanofiber-Based Cartilage Tissue Engineering Using Improved Cell Seeding, Growth Factor, and Bioreactor Technologies." Tissue Engineering Part A **14**(5): 639-648.

Li, W., R. Mauck, et al. (2005). "Electrospun nanofibrous scaffolds: production, characteriation, and applications for tissue engineering and drug delivery." J Biomed Nanotechnol **1**: 259-275.

Li, W. J., K. G. Danielson, et al. (2003). "Biological response of chondrocytes cultured in three-dimensional nanofibrous poly(epsilon-caprolactone) scaffolds." J Biomed Mater Res A **67**(4): 1105-14.

Li, W. J., Y. J. Jiang, et al. (2006). "Chondrocyte phenotype in engineered fibrous matrix is regulated by fiber size." Tissue Eng **12**(7): 1775-85.

Li, W. J., C. T. Laurencin, et al. (2002). "Electrospun nanofibrous structure: a novel scaffold for tissue engineering." J Biomed Mater Res **60**(4): 613-21.

Li, W. J., R. L. Mauck, et al. (2007). "Engineering controllable anisotropy in electrospun biodegradable nanofibrous scaffolds for musculoskeletal tissue engineering." J Biomech **40**(8): 1686-93.

Li, W. J., R. Tuli, et al. (2005). "Multilineage differentiation of human mesenchymal stem cells in a three-dimensional nanofibrous scaffold." Biomaterials **26**(25): 5158-66.

Li, W. J., R. Tuli, et al. (2005). "A three-dimensional nanofibrous scaffold for cartilage tissue engineering using human mesenchymal stem cells." Biomaterials **26**(6): 599-609.

Liao, I. C., S. Chen, et al. (2009). "Sustained viral gene delivery through core-shell fibers." Journal of Controlled Release **139**(1): 48-55.

Liao, I. C., S. Y. Chew, et al. (2006). "Aligned core-shell nanofibers delivering bioactive proteins." Nanomedicine **1**(4): 465-471.

Little, D., F. Guilak, et al. "Ligament-derived matrix stimulates a ligamentous phenotype in human adipose-derived stem cells." Tissue Eng Part A **16**(7): 2307-19.

Luong-Van, E., L. Grondahl, et al. (2006). "Controlled release of heparin from poly(epsilon-caprolactone) electrospun fibers." Biomaterials **27**(9): 2042-2050.

Mak, A. F. (1986). "The Apparent Viscoelastic Behavior of Articular Cartilage---The Contributions From the Intrinsic Matrix Viscoelasticity and Interstitial Fluid Flows." Journal of Biomechanical Engineering **108**(2): 123-130.

Matthews, J. A., G. E. Wnek, et al. (2002). "Electrospinning of collagen nanofibers." Biomacromolecules **3**(2): 232-8.

Mauck, R. L., B. M. Baker, et al. (2009). "Engineering on the Straight and Narrow: The Mechanics of Nanofibrous Assemblies for Fiber-Reinforced Tissue Regeneration." Tissue Eng Part B Rev **15**(2): 171-93.

Mauney, J. R., T. Nguyen, et al. (2007). "Engineering adipose-like tissue in vitro and in vivo utilizing human bone marrow and adipose-derived mesenchymal stem cells with silk fibroin 3D scaffolds." Biomaterials.

McCullen, S. D., Y. Zhu, et al. (2009). "Electrospun composite poly(L-lactic acid)/tricalcium phosphate scaffolds induce proliferation and osteogenic differentiation of human adipose-derived stem cells." Biomed Mater **4**(3): 35002.

Moutos, F. T., L. E. Freed, et al. (2007). "A biomimetic three-dimensional woven composite scaffold for functional tissue engineering of cartilage." Nat Mater **6**(2): 162-7.

Mow, V. C., G. A. Ateshian, et al. (1993). "Biomechanics of Diarthrodial Joints: A Review of Twenty Years of Progress." Journal of Biomechanical Engineering **115**(4B): 460-467.

Mow, V. C. and X. E. Guo (2002). "Mechano-electrochemical properties of articular cartilage: their inhomogeneities and anisotropies." Annu Rev Biomed Eng **4**: 175-209.

Mow, V. C. and R. Huiskes (2005). Basic Orthopaedic Biomechanics and Mechano-Biology.

Mow, V. C., S. C. Kuei, et al. (1980). "Biphasic Creep and Stress Relaxation of Articular Cartilage in Compression: Theory and Experiments." Journal of Biomechanical Engineering **102**: 73-84.

Mow, V. C., A. Ratcliffe, et al. (1992). "Cartilage and diarthrodial joints as paradigms for hierarchical materials and structures." Biomaterials **13**(2): 67-97.

Nam, J., Y. Huang, et al. (2007). "Improved Cellular Infiltration in Electrospun Fiber via Engineered Porosity." Tissue Engineering **13**(9): 2249-2257.

Nerurkar, N. L., B. M. Baker, et al. (2006). "Engineering of fiber-reinforced tissues with anisotropic biodegradable nanofibrous scaffolds." Conf Proc IEEE Eng Med Biol Soc **1**: 787-90.

Nerurkar, N. L., B. M. Baker, et al. (2009). "Nanofibrous biologic laminates replicate the form and function of the annulus fibrosus." Nat Mater **8**(12): 986-992.

Nerurkar, N. L., D. M. Elliott, et al. (2007). "Mechanics of oriented electrospun nanofibrous scaffolds for annulus fibrosus tissue engineering." Journal of Orthopaedic Research **25**(8): 1018-1028.

NIAMS. (2011). "Handout on Health: Osteoarthritis." 2010, from http://www.niams.nih.gov/Health_Info/Osteoarthritis/default.asp.

Pfaffl, M. W. (2001). "A new mathematical model for relative quantification in real-time RT-PCR." Nucleic Acids Res **29**(9): e45.

Pham, Q. P., U. Sharma, et al. (2006). "Electrospinning of polymeric nanofibers for tissue engineering applications: a review." Tissue Eng **12**(5): 1197-211.

Pham, Q. P., U. Sharma, et al. (2006). "Electrospun Poly(ε–caprolactone) Microfiber and Multilayer Nanofiber/Microfiber Scaffolds: Characterization of Scaffolds and Measurement of Cellular Infiltration." Biomacromolecules **7**(10): 2796-2805.

Ramakrishna, S., K. Fujihara, et al. (2005). An Introduction to Electrospinning and Nanofibers. Singapore, World Scientific Publishing Co. Pte. Ltd.

Rasband, W. S. (1997-2011). ImageJ. U.S. National Institues of Health, Bethesda, Maryland, USA, http://imagej.nih.gov/ij/.

Reneker, D. H., A. L. Yarin, et al. (2000). "Bending instability of electrically charged liquid jets of polymer solutions in electrospinning." Journal of Applied Physics **87**(9): 4531-4547.

Sanders, J. E., D. V. Cassisi, et al. (2003). "Relative influence of polymer fiber diameter and surface charge on fibrous capsule thickness and vessel density for single-fiber implants." J Biomed Mater Res A **65**(4): 462-7.

Sanders, J. E., C. E. Stiles, et al. (2000). "Tissue response to single-polymer fibers of varying diameters: evaluation of fibrous encapsulation and macrophage density." J Biomed Mater Res **52**(1): 231-7.

Sell, S. A., P. S. Wolfe, et al. (2011). "Incorporating Platelet-Rich Plasma into Electrospun Scaffolds for Tissue Engineering Applications." Tissue Eng Part A.

Shields, K. J., M. J. Beckman, et al. (2004). "Mechanical properties and cellular proliferation of electrospun collagen type II." Tissue Engineering **10**(9-10): 1510-1517.

Shin, M., H. Yoshimoto, et al. (2004). "In vivo bone tissue engineering using mesenchymal stem cells on a novel electrospun nanofibrous scaffold." Tissue Eng **10**(1-2): 33-41.

Steadman, J. R., W. G. Rodkey, et al. (2001). "Microfracture: Surgical Technique and Rehabilitation to Treat Chondral Defects." Clinical Orthopaedics and Related Research **391**: S362-S369.

Stella, J. A., J. Liao, et al. (2008). "Tissue-to-cellular level deformation coupling in cell micro-integrated elastomeric scaffolds." Biomaterials **29**(22): 3228-3236.

Sun, H. F., L. Mei, et al. (2006). "The in vivo degradation, absorption and excretion of PCL-based implant." Biomaterials **27**(9): 1735-1740.

Taylor, G. (1964). "Disintegration of Water Drops in an Electric Field." Proceedings of the Royal Society of London. Series A, Mathematical and Physical Sciences **280**(1382): 383-397.

Taylor, G. (1969). "Electrically Driven Jets." Proceedings of the Royal Society of London. Series A, Mathematical and Physical Sciences **313**(1515): 453-475.

Tzezana, R., E. Zussman, et al. (2008). "A Layered Ultra-Porous Scaffold for Tissue Engineering, Created via a Hydrospinning Method." Tissue Eng Part C Methods **14**(4): 281-288.

Urist, M. R. (1965). "Bone: Formation by Autoinduction." Science **150**(3698): 893-899.

Verteramo, A. and B. B. Seedhorn (2004). "Zonal and directional variations in tensile properties of bovine articular cartilage *with special reference to strain rate variation*." Biorheology **41**(3-4): 203-213.

Woo, S. L. Y., W. H. Akeson, et al. (1976). "Measurements of nonhomogeneous, directional mechanical properties of articular cartilage in tension." Journal of Biomechanics **9**(12): 785-791.

Wood, J. J., M. A. Malek, et al. (2006). "Autologous cultured chondrocytes: adverse events reported to the United States Food and Drug Administration." J Bone Joint Surg Am **88**(3): 503-7.

Xie, J., X. Li, et al. (2008). "Putting Electrospun Nanofibers to Work for Biomedical Research." Macromol Rapid Commun **29**(22): 1775-1792.

Yang, F., R. Murugan, et al. (2005). "Electrospinning of nano/micro scale poly(L-lactic acid) aligned fibers and their potential in neural tissue engineering." Biomaterials **26**(15): 2603-2610.

Yim, E. K. F., R. M. Reano, et al. (2005). "Nanopattern-induced changes in morphology and motility of smooth muscle cells." Biomaterials **26**(26): 5405-5413.

Yin, Z., X. Chen, et al. "The regulation of tendon stem cell differentiation by the alignment of nanofibers." Biomaterials **31**(8): 2163-2175.

Yoshimoto, H., Y. M. Shin, et al. (2003). "A biodegradable nanofiber scaffold by electrospinning and its potential for bone tissue engineering." Biomaterials **24**(12): 2077-2082.

Zhang, Y. Z., J. Venugopal, et al. (2005). "Characterization of the Surface Biocompatibility of the Electrospun PCL-Collagen Nanofibers Using Fibroblasts." Biomacromolecules **6**(5): 2583-2589.

Zhong, S. P., W. E. Teo, et al. (2005). "Formation of collagen-glycosaminoglycan blended nanofibrous scaffolds and their biological properties." Biomacromolecules **6**(6): 2998-3004.

Zhong, S. P., W. E. Teo, et al. (2007). "Development of a novel collagen-GAG nanofibrous scaffold via electrospinning." Materials Science and Engineering: C **27**(2): 262-266.

Zong, X., H. Bien, et al. (2005). "Electrospun fine-textured scaffolds for heart tissue constructs." Biomaterials **26**(26): 5330-5338.

# Biography

Ned William Garrigues II
Born April 10, 1982, Portsmouth, VA
B.A., Engineering Sciences, Harvard University, Cambridge, MA
Biomedical concentration, magna cum laude, 2004

**Publications:**

Use of an insulating mask for controlling anisotropy in multilayer electrospun scaffolds for tissue engineering. **Garrigues NW**, Little D, O'Conor CJ, Guilak F. *J Materials Chemistry* 2010 Oct 28; 20(40): 8962-8968.

Can locking screws allow small, low-profile plates to achieve comparable stability to larger, standard plates? Garrigues GE, Glisson RR, **Garrigues NW**, Richard MJ, Ruch DS. *J Orthopaedic Trauma*. 2011 Jun;25(6):347-54.

U.S. Patent No. 61/163,307 for "Unified Plate Construct System and Method", 2009.

Estrogen and LH dynamics during the follicular phase of the estrous cycle in the Asian elephant. Czekala, N., E. MacDonald, K. Steinman, S. Walker, N. Garrigues, D. Olson, and J. Brown (2003). Zoo Biology 22:443-454.

**Presentations:**

Anisotropic Electrospun Scaffolds for Tissue Engineering: Fiber Alignment and its Effect on Cells. **Will Garrigues**, Dianne Little, Chris O'Conor, Ian Gao, Farshid Guilak. Gordon Research Conference: Musculoskeletal Biology & Bioengineering, Andover, NH, Aug. 1-6, 2010. (poster)

A Novel Method for Producing Anisotropic Electrospun Polymer Scaffolds for Tissue Engineering. **Will Garrigues**, Jason Klein, Ian Gao, Franklin T. Moutos, Farshid Guilak. (poster)

Electrospun Scaffolds for Tissue Engineering. **Will Garrigues**. Society of Duke Fellows, Mar. 17, 2009. (invited talk)

Anisotropic Electrospun Polymer Scaffolds for Tissue Engineering. **Will Garrigues**, Jason Klein, Syrone Liu, Franklin T. Moutos, Robert T. Clark, and Farshid Guilak. (poster)

Electrohydrodynamic Processing of Functional Biomedical Scaffolds. Syrone Liu, **Will Garrigues**, Yiquan Wu, Farshid Guilak, Rob Clark. (poster)

**Grants, Fellowships, Awards and Honors**

Center for Biomolecular and Tissue Engineering Fellow (2006-2008)
James B. Duke Scholar (2005-present)
Duke Endowment Scholar (2005-2006)
Duke Biomedical Engineering Dept. Retreat, 2nd place poster, 2010.